Anaerobic treatment of sulfate-rich wastewaters: process modeling and control

A. Robles, S. Vinardell, J. Serralta, N. Bernet, P. N L Lens, Jean-Philippe P Steyer, S. Astals

Chapter 9

Anaerobic treatment of sulfate-rich wastewaters: process modeling and control

A. Robles, S. Vinardell, J. Serralta, N. Bernet, P. N. L. Lens, J. P. Steyer and S. Astals

9.1 INTRODUCTION

A variety of anthropogenic activities, especially at industrial level, generate wastewater streams rich in sulfate which, if improperly treated, can cause health, social and environmental problems (Serrano *et al.*, 2020). These industrial activities include food production (e.g. edible oil, seafood-processing), fermentation industry, tanneries, coal-burning power plants, paper and pulp industry, mining and metallurgical processes. Additionally, in some regions (e.g. Hong Kong), the use of seawater for toilet flushing to alleviate the pressure on potable water has increased the sulfate concentration in municipal sewage (Li *et al.*, 2018; Wu *et al.*, 2016).

Anaerobic digestion (AD) is a well-established technology to transform municipal and industrial organic-rich wastewaters into renewable energy in the form of methane-rich biogas. Besides energy recovery, AD presents other important advantages compared to aerobic treatment such as low sludge production and low energy requirements (Puyol *et al.*, 2017). AD is also a suitable technology to treat organic-rich municipal and industrial wastewaters containing sulfate. However, a high sulfate content can affect the AD process performance and feasibility due to (i) the competition for easily biodegradable organic matter (e.g. short chain fatty acids, hydrogen) between sulfate reducers and anaerobic microorganisms (Cassidy *et al.*, 2015; Kalyuzhnyi *et al.*, 1998), (ii) the generation of H_2S, the product of sulfate

DOI: 10.2166/9781789060959_0277

reduction, which is malodorous, toxic, and corrosive. H_2S can damage the combined heat and power (CHP) unit and metal parts of the infrastructure (e.g. gas storage tanks, compressors, and pipelines) by itself or through SO_2 formation from combustion (H_2SO_4 when combined with the biogas moisture), which requires equipment and instrumentation resistant to corrosion (Angelidaki *et al.*, 2018), and (iii) the inhibitory impact of H_2S on anaerobic microorganisms since H_2S is a lipophilic compound that can diffuse through the microbial cell membrane and damage cellular metabolism (Chen *et al.*, 2008; Li & Lancaster, 2013). The detrimental impact of H_2S on the AD process and infrastructure requires the effective prediction and control of the H_2S concentration in the biogas and in the digestion liquor.

Several mathematical models have been developed to model the sulfur cycling in anaerobic biotechnologies, primarily for continuous stirred tank reactor (CSTR) and upflow anaerobic sludge blanket (UASB) systems, but also for batch and plug flow systems (Cassidy *et al.*, 2015; Knobel & Lewis, 2002). The sulfur cycling is quite complex since it is metabolically diverse and it is connected to the carbon, nitrogen, phosphorus and iron cycles among others. Most models have focused on the substrate competition between sulfate-reducing bacteria and anaerobic microorganisms (including acetogenic bacteria and methanogenic archaea) and the inhibition of anaerobic microorganisms by hydrogen sulfide. Some models have also incorporated sulfide precipitation (Flores-Alsina *et al.*, 2016; Gupta *et al.*, 1994).

Anaerobic reactors treating sulfate-rich streams can be very unstable (see Chapter 6). Therefore, implementing an efficient monitoring and control system is required to keep the process running adequately. The monitoring and control system is particularly important in the presence of a fluctuating input pollution and/or when the influent has a low biological oxygen demand (BOD) to sulfate ratio. Different types of sensors are available for providing the on-line data required for sulfate reduction process control, such as chemical sensors and analyzers, microsensors or biosensors (Cassidy *et al.*, 2015). The combination of these sensors with molecular techniques would allow monitoring of microbial activity and microbial ecology in bioreactors where sulfate reduction occurs. This would be useful for development of a control strategy considering sulfide production as a control parameter.

This chapter reviews the current state-of-the-art models, monitoring techniques and control strategies applied to anaerobic processes for sulfate-rich wastewater treatment.

9.2 MODELS

Dynamic mathematical models are powerful tools to improve the understanding, monitoring, and control of wastewater treatment plants and anaerobic digesters

(Batstone *et al.*, 2015; Jimenez *et al.*, 2015; Olsson *et al.*, 2014; Solon *et al.*, 2017). The power of mathematical models lies in their capacity to reproduce an empirical behavior on a computer, in a clear and quantifiable manner, where the mathematical equations simulate the physical, chemical, and biological processes. Mathematical models can be used to analyze, predict and optimize the performance of a process or plant under different operating conditions which is a useful tool to complement and improve lab- and pilot-scale studies (Fernández-Arévalo *et al.*, 2017; Lizarralde *et al.*, 2019; Seco *et al.*, 2020). Mathematical models can also help to understand the process from a global point of view and to train process operators. For instance, Kazadi Mbamba *et al.* (2019) analyzed the plant-wide impact of different iron dosages for chemical phosphorus removal, Martí *et al.* (2017) modeled different sludge management strategies in a wastewater treatment plant (WWTP) to enhance phosphorus recovery, and Arnell *et al.* (2016) modeled the plant-wide impact of different co-digestion strategies. Last but not least, simplified mathematical models are used in the control loop to improve process operation.

The dynamic modeling of AD and/or sulfate reduction processes has been largely reported in the literature due to the importance of these biotechnologies in the development of the circular economy (Batstone *et al.*, 2002, 2006; Fedorovich *et al.*, 2003; Lauwers *et al.*, 2013). A comprehensive review of the kinetic parameters related to the sulfur cycle in these models (e.g. maximum specific uptake rate, half-saturation constant, microbial growth yield, decay rate, inhibition function and constants, Henry's law coefficient, p*K*a dissociation value) can be found in Barrera *et al.* (2013) and Cassidy *et al.* (2015). In a recent publication, Ahmed and Rodríguez (2018) carried out a comparative study of five different structures of sulfate reduction models for AD to find a trade-off between model complexity and model accuracy.

9.2.1 Models at reactor level

Pioneering publications dealing with sulfate reduction were published in the 1990s (Gupta *et al.*, 1994; Vavilin *et al.*, 1994), and publications dealing with this topic have been steadily published ever since. The publication of the Anaerobic Digestion Model N°1 (ADM1) (Batstone *et al.*, 2002) represented a breakthrough for anaerobic biotechnologies modeling since it created a common basis for further model development and validation studies. ADM1 also aimed to make model outcomes more comparable and compatible, as well as to assist a technology transfer from research to industry (Batstone *et al.*, 2002). The original ADM1 only included organic and inorganic carbon and nitrogen reactions and did not include sulfur transformations due to the complexity of the sulfur cycle. However, publications including sulfur transformation with the ADM1 model appeared soon after its publication (Batstone *et al.*, 2006; Fedorovich *et al.*, 2003).

Since then, several models have been developed to describe sulfate reduction, either through standalone models or by incorporating sulfate reduction into ADM1 (Ahmed & Rodríguez, 2018). The sulfur cycle involves several biochemical and physical processes which have been incorporated in the models to different degrees depending on the assumptions and the framework of the study. The processes associated with sulfur include: (i) heterotrophic and/or autotrophic sulfate reduction to sulfide, which is linked to sulfate-reducing bacteria (SRB) biomass growth, (ii) SRB biomass decay, (iii) hydrogen sulfide inhibition to anaerobic microorganisms, (iv) sulfide speciation in the liquid phase (i.e. acid-base chemistry), (v) hydrogen sulfide liquid-gas mass transfer, (vi) precipitation of metal sulfides, and (vii) the uptake and release of inorganic sulfur due to biomass growth and decay. The latter has not been included in any model due to the relatively small sulfur concentration in organic molecules. Consequently, it will not be discussed in this chapter.

9.2.1.1 Stoichiometry and kinetics of sulfate reduction

Sulfate-reducing bacteria (SRB) can utilize a wide variety of compounds as electron donors such as alcohols (e.g. methanol and ethanol), organic acids (e.g. formate, lactate, acetate, propionate, butyrate, pyruvate and malate), aromatic compounds (e.g. benzoate and phenol), and hydrogen (Muyzer & Stams, 2008). Thus, sulfate reduction can be carried out by heterotrophic and autotrophic SRB. Heterotrophic SRB use organic compounds as an electron donor and carbon source, while autotrophic SRB use H_2 as an electron donor and CO_2 as a carbon source (Lens & Kuenen, 2001; Muyzer & Stams, 2008). Figure 9.1 shows a schematic representation of the biochemical processes included in the model ADM1, including the sulfate-reducing processes modeled by different authors at different complexity levels. Acetate, propionate and butyrate are the most common organic substrates for SRB in these models since they are intermediate compounds of the AD process. Lactate has also been incorporated in a few models (D'Acunto *et al.*, 2011; Knobel & Lewis, 2002). However, lactate concentrations in anaerobic digesters are low compared to volatile fatty acids concentrations and, consequently, it has been generally omitted. The degradation of butyrate and propionate by SRB can be complete (the carbon source is oxidized to CO_2) or incomplete (the carbon source is oxidized to acetate). The incomplete oxidation of alcohols, lactate and fatty acids by SRB appears as the most common degradation pathway (Muyzer & Stams, 2008) and, therefore, this is the utilized pathway to achieve a more realistic and more flexible model (Barrera *et al.*, 2013; Fedorovich *et al.*, 2003). However, some models have also incorporated the complete oxidation of these compounds (Cassidy *et al.*, 2015; D'Acunto *et al.*, 2011; Gupta *et al.*, 1994; Knobel & Lewis, 2002). Autotrophic sulfate reduction has been included in most models. The stoichiometry of the

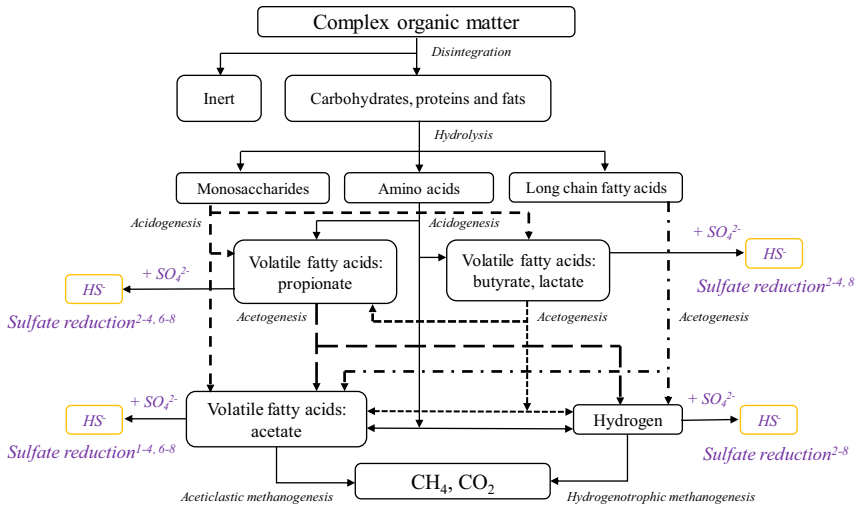

Figure 9.1 Schematic representation of the biochemical processes included in the model ADM1, including sulfate-reducing processes modeled by different authors (adapted from Robles *et al.* (2018)). [1]Fomichev and Vavilin (1997); [2]Kalyuzhnyi *et al.* (1998); [3]Knobel and Lewis (2002); [4]Fedorovich *et al.* (2003); [5]Frunzo *et al.* (2012); [6]Durán (2013); Durán *et al.* (2017); [7]Barrera *et al.* (2015); [8]Ahmed and Rodríguez (2018).

SRB reactions including incomplete heterotrophic and autotrophic sulfate reduction are:

- Butyric acid incomplete oxidation

$$2CH_3CH_2CH_2COOH + H_2SO_4 \rightarrow 4CH_3COOH + H_2S$$

- Propionic acid incomplete oxidation

$$4CH_3CH_2COOH + 3H_2SO_4 \rightarrow 4CH_3COOH + 4CO_2 + 4H_2O + 3H_2S$$

- Lactic acid incomplete oxidation

$$2CH_3CHOHCOOH + H_2SO_4 \rightarrow 2CH_3COOH + 2CO_2 + 2H_2O + H_2S$$

- Acetic acid oxidation

$$CH_3CH_2COOH + H_2SO_4 \rightarrow 2CO_2 + 2H_2O + H_2S$$

- Hydrogen oxidation

$$4H_2 + H_2SO_4 \rightarrow 4H_2O + H_2S$$

Sulfate reduction kinetics are commonly modeled by dual-substrate Monod kinetics, representing either the SRB growth rate (Equation 9.1) or the SRB substrate uptake rate (Equation 9.2). These equations are linked since the maximum specific uptake rate (k_m) is obtained by dividing the maximum specific growth rate (μ_{max}) by the biomass yield (Y) (i.e. $k_m = \mu_{max}/Y$) (Barrera *et al.*, 2013). Both approaches have been used to model sulfate reduction, however, anaerobic models normally focus on catabolism (i.e. substrate consumption, Equation 9.2) rather than on anabolism (i.e. biomass growth, Equation 9.1). Note that the activated sludge models used to model carbon, nitrogen and phosphorus removal under aerobic and anoxic conditions focus on anabolism due to the higher biomass yield under these conditions (Henze *et al.*, 2006). The dual-substrate Monod equations (Equation 9.1 and 9.2) have one term for the electron donor (organic carbon or hydrogen) and one term for the electron acceptor (sulfate). Each of these terms act as a switching function, which "on/off" the reaction depending on the electron donor or electron acceptor availability. Sulfate reduction models incorporate a dual-term Monod equation for each niche of SRB (iSRB), based on the electron donor utilized to carry out sulfate reduction:

$$\rho_{\text{growth},i} = \mu_{\text{max,iSRB}} \cdot \frac{S_i}{K_{S,\text{iSRB}} + S_i} \cdot \frac{S_{SO_4}}{K_{S,SO_4,\text{iSRB}} + S_{SO_4}} \cdot X_{\text{iSRB}} \tag{9.1}$$

$$\rho_{\text{uptake},i} = k_{m,\text{iSRB}} \cdot \frac{S_i}{K_{S,\text{iSRB}} + S_i} \cdot \frac{S_{SO_4}}{K_{S,SO_4,\text{iSRB}} + S_{SO_4}} \cdot X_{\text{iSRB}} \tag{9.2}$$

In Equation 9.2, $k_{m,\text{iSRB}}$ is the maximum specific uptake rate of iSRB biomass, S_i is the electron donor i concentration, $K_{S,\text{iSRB}}$ is the half-saturation constant of iSRB biomass towards the electron donor, S_{SO4} is the sulfate concentration, $K_{S,SO4,\text{iSRB}}$ is the half-saturation constant of iSRB biomass towards sulfate, and X_{iSRB} is the iSRB biomass concentration.

The number of SRB in existing models varies from two (Harerimana *et al.*, 2013; Vavilin *et al.*, 1994) to five (Knobel & Lewis, 2002), although three and four SRB types are the most common approaches, including butyrate-utilizing SRB (bSRB), propionate-utilizing SRB (pSRB), acetate-utilizing SRB (aSRB) and hydrogen-utilizing SRB (hSRB) (Fedorovich *et al.*, 2003; Flores-Alsina *et al.*, 2016). Acetate- and hydrogen-utilizing SRB have been incorporated in most models, which is expected considering that acetate and hydrogen are the final intermediates before methanogenesis and that, under stable conditions, fermentation reactions are relatively fast compared to methanogenesis (Ahmed & Rodríguez, 2018; Peces *et al.*, 2018). Accordingly, some researchers omitted butyrate-utilizing SRB in their models (Barrera *et al.*, 2015; Poinapen & Ekama, 2010). However, propionate-utilizing SRB should not be omitted, since propionate degradation is the least thermodynamically favorable reaction among short chain fatty acids fermentation. Propionate degradation has been reported

to be influenced by changes in hydrogen concentration, microbial inhibition and process disturbances (Ito *et al.*, 2012; Yang *et al.*, 2015). Regarding hydrogen-utilizing SRB, Batstone *et al.* (2006) pointed out that for influents with low sulfate concentrations, hydrogen-utilizing SRB would be the dominant sulfate reduction pathway and, to reduce the model complexity, it should be the only sulfate reduction reaction considered in the model. However, at higher influent sulfate concentrations, volatile-fatty-acid-utilizing SRB could be significant and, therefore, they need to be included in the model.

9.2.1.2 Endogenous respiration of sulfate reduction bacteria

Endogenous respiration (i.e. biomass decay) has been included in most models. The first-order function (Equation 9.3) has been used to model endogenous respiration of biomass since pioneering models were developed (Gupta *et al.*, 1994). Later on, it was stablished as the default equation to model biomass decay in the ADM1 (Batstone *et al.*, 2002):

$$\rho_{\text{decay,iSRB}} = k_{d,\text{iSRB}} \cdot X_{\text{iSRB}} \tag{9.3}$$

where $k_{d,\text{iSRB}}$ is the first-order decay rate constant of iSRB biomass and X_{iSRB} is the concentration of iSRB biomass.

9.2.1.3 Inhibition by hydrogen sulfide

Substrate competition between sulfate-reducing bacteria, fermenters, and methanogenic microorganisms is controlled by the maximum specific uptake rate (k_m) and the half-saturation constant (K_S) of the microorganisms involved. However, the sensitivity of the different microorganisms towards inhibition can have a strong impact on the overall process performance by decreasing the substrate uptake rate (Cassidy *et al.*, 2015). The ADM1 included pH inhibition for all microorganisms, hydrogen inhibition from acetogenic microorganisms (i.e. valerate, butyrate and propionate degraders) and free ammonia inhibition from acetoclastic methanogens. H_2S inhibition was not included, since sulfate reduction was not included (Batstone *et al.*, 2002). However, hydrogen sulfide inhibition has been included in most models including sulfate reduction (Ahmed & Rodríguez, 2018; Fedorovich *et al.*, 2003). Inhibition is implemented in the model by including an inhibition term for each inhibitor to the uninhibited Monod equation. For instance, the inclusion of an inhibition term for H_2S inhibition expands Equation 9.2 to Equation 9.4, where $I_{\text{h2s,iSRB}}$ varies from 1 (no-inhibition) to 0 (complete inhibition) as the inhibitor concentration increases:

$$\rho_{\text{uptake},i} = k_{m,\text{iSRB}} \cdot \frac{S_i}{K_{S,\text{iSRB}} + S_i} \cdot \frac{S_{\text{SO}_4}}{K_{S,\text{SO}_4,\text{iSRB}} + S_{\text{SO}_4}} \cdot X_{\text{iSRB}} \cdot I_{\text{h2s,iSRB}} \tag{9.4}$$

The inhibition term ($I_{h2s,iSRB}$) has an inhibition function that determines the relationship between the inhibitor concentration and the decrease in the specific substrate utilization rate. The non-competitive inhibition function is the most utilized function to describe H_2S inhibition in these models (Equation 9.5); likely because it was the default inhibition function in the ADM1 (Barrera *et al.*, 2015; Flores-Alsina *et al.*, 2016; Knobel & Lewis, 2002; Sun *et al.*, 2016). Nonetheless, other inhibition functions have been used as well (Equations 9.5–9.7). Inhibition functions used to model H_2S inhibition include:

- Non-competitive inhibition function:

$$I_{h2s,iSRB} = \frac{K_{I,h2s,iSRB}}{K_{I,h2s,iSRB} + S_{h2s}} \tag{9.5}$$

  where $K_{I,h2s,iSRB}$ is the 50% inhibitory constant of H_2S on biomass iSRB, and S_{h2s} is the H_2S concentration in the liquid phase.
- First-order inhibition function (Fedorovich *et al.*, 2003; Kalyuzhnyi *et al.*, 1998):

$$I_{h2s,iSRB} = \begin{cases} \left(\dfrac{K_{I,h2s,iSRB} - S_{h2s}}{K_{I,h2s,iSRB}}\right)_{S_{h2S} \le K_I} \\ 0 \quad _{S_{h2S} > K_I} \end{cases} \tag{9.6}$$

  where $K_{I,h2s,iSRB}$ represents the H_2S concentration at which iSRB is 100% inhibited, and S_{h2s} is the H_2S concentration in the liquid phase.
- Modified non-competitive inhibition function (so-called 2×2 constants) (Vavilin *et al.*, 1995):

$$I_{h2s,iSRB} = \frac{1}{1 + \left(\dfrac{S_{h2s}}{K_{100}}\right)^{\dfrac{\ln 99}{\ln\left(\dfrac{K_2}{K_{100}}\right)}}} \tag{9.7}$$

  where K_2 represents the H_2S concentration at which the rate of iSRB is decreased by half, K_{100} represents the H_2S concentration at which the rate of iSRB is decreased one hundred times, and S_{h2s} is the H_2S concentration in the liquid phase.
- Poinapen and Ekama inhibition function (Poinapen & Ekama, 2010):

$$I_{h2s,iSBR} = \exp\left[-\left(\frac{S_{h2s}}{1.20112 \cdot K_{I,h2s,iSBR}}\right)^2\right] \tag{9.8}$$

  where $K_{I,h2s,iSRB}$ is the 50% inhibitory concentration of H_2S on biomass iSRB and S_{h2s} is the H_2S concentration in the liquid phase.

Although each inhibition function has a distinctive profile (see Figure 9.2), most publications did not justify the selection of a specific inhibition function. The key difference between the non-competitive inhibition function (Equation 9.5) and the other inhibition functions (Equations 9.6–9.8) is that in the non-competitive inhibition functions, inhibition is not complete ($I_{h2s,iSRB} = 0$) even at extremely high inhibitor concentrations ($I_{h2s,iSRB} = 0.09$ at 100 mg H_2S-S $\cdot$ L^{-1} for a $K_{I,h2s,iSRB}$ of 10 mg H_2S-S $\cdot$ L^{-1}). On the other hand, there is a high uniformity regarding the microorganisms inhibited by H_2S in these models, where H_2S inhibition has been applied to all AD microorganisms that compete with SRB for the electron donors (e.g. butyrate-degraders, propionate-degraders, lactate-degraders, acetoclastic methanogens, and hydrogenotrophic methanogens) as well as all SRB groups included in the model. Ahmed and Rodríguez (2018) compared the inhibition parameters reported in several publications and found notable consistency among them. Differences between inhibition parameters are approximately two-fold, which can be considered a low variability considering the different experimental conditions and model structures from which these parameters were obtained. However, it should be noted that these parameters were obtained from different equations, which limits transportability among studies.

9.2.1.4 Acid-base equilibria

The inhibition function (Equations 9.5–9.8) uses the free H_2S concentration as the inhibitory agent, since H_2S has been reported to be more inhibitory than HS^- and

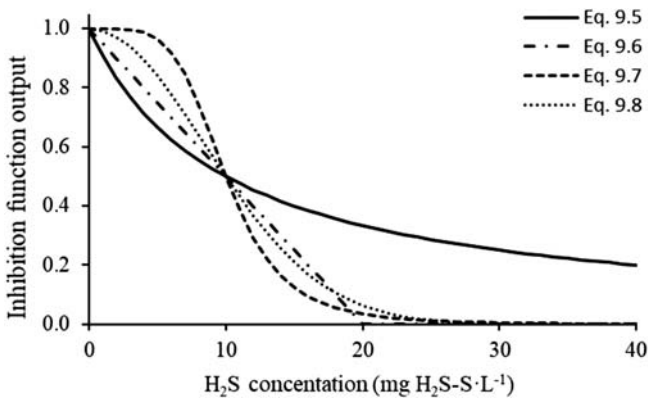

Figure 9.2 Profile of the different inhibition functions utilized to model H_2S inhibition for a 50% inhibitory concentration of 10 mg H_2S-S $\cdot$ L^{-1}. Solid line represents the non-competitive inhibition function. Dash-dotted line represents the first-order inhibition function. Dashed line represents Vavilin *et al.* (1995) inhibition function [K_{100} was set at 26 mg H_2S-S $\cdot$ L^{-1} for comparison purposes since this was the concentration that reduced the rate 100 times in Equation 9.7]. Dotted line represents the Poinapen and Ekama (2010) inhibition function.

S^{2-} (Chen *et al.*, 2008). Therefore, models need to include sulfide acid-base chemistry to resolve sulfide speciation in the liquid phase and to properly describe H_2S inhibition. Nonetheless, sulfide speciation is required to model the pH and the ionic strength of the liquid phase, H_2S liquid-gas mass transfer, and ion pairing for precipitation (Flores-Alsina *et al.*, 2016; Knobel & Lewis, 2002; Solon *et al.*, 2015).

$$H_2S_{(aq)} \underset{pK_{a1}}{\longleftrightarrow} HS^{\mp}H^{+} \underset{pK_{a2}}{\longleftrightarrow} S^{2-} + 2H^{+} \tag{9.9}$$

H_2S is a diprotic acid since it has two hydrogen atoms that can dissociate in its molecule (Equation 9.9). H_2S is a weak acid with a pK_{a1} of 7.01 and pK_{a2} of 13.8 at 25°C (Millero, 1986). However, there is some uncertainty in the literature regarding these values, since reported pK_{a1} values at 25°C range from 6.97 to 7.06, while pK_{a2} values vary from 12.2 to 15.0 (Li & Lancaster, 2013; Millero, 1986). Biological reactors are operated around neutral or slightly acidic pH. Consequently, in most models only the H_2S and HS^- concentration have been included since the S^{2-} concentration was assumed negligible (Barrera *et al.*, 2013; Fedorovich *et al.*, 2003). Sulfide speciation can be calculated using Equations 9.10–9.12:

$$S_{h2s} = \frac{(S_{h+})^2 \cdot S_{IS}}{(S_{h+})^2 + S_{h+} \cdot K_{a1} + K_{a1} \cdot K_{a2}} \approx \frac{S_{h+} \cdot S_{IS}}{K_{a1} + S_{h+}} \tag{9.10}$$

$$S_{hs-} = \frac{S_{h+} \cdot K_{a1} \cdot S_{IS}}{(S_{h+})^2 + S_{h+} \cdot K_{a1} + K_{a1} \cdot K_{a2}} \approx \frac{K_{a1} \cdot S_{IS}}{K_{a1} + S_{h+}} \tag{9.11}$$

$$S_{s2-} = \frac{K_{a1} \cdot K_{a2} \cdot S_{IS}}{(S_{h+})^2 + S_{h+} \cdot K_{a1} + K_{a1} \cdot K_{a2}} \approx 0 \tag{9.12}$$

where S_{h+} is the protons concentration, S_{IS} is the total sulfur concentration (IS stands for inorganic sulfur), K_{a1} is the first acid-base equilibrium constant of H_2S, and K_{a2} is the second acid-base equilibrium constant of H_2S.

Anaerobic digesters and sulfate reducing reactors are frequently operated at mesophilic conditions (35°C) (Serrano *et al.*, 2020), which reduces the pK_{a1} values from 7.0 to 6.8 (Hughes *et al.*, 2009; Millero, 1986). The impact of temperature on the acid dissociation constant has not been considered in most models, however, at mesophilic conditions (~35°C) the calculated free H_2S concentration in the liquid phase is 20–30% lower (depending on the digester pH) than at 25°C. The van 't Hoff equation (Equation 9.13) is the function recommended in ADM1 to describe the variation of equilibrium constants with temperature (where the pK_{a1} was 7.04 at 298 K and θ was 0.029), which provides similar pK_{a1} values to the empirical equations in Millero (1986):

$$K_{a,T_2} = K_{a,T_1} \cdot e^{\theta(T_2 - T_1)} \tag{9.13}$$

Finally, when the inorganic sulfur species in the model are solved using ODE (ordinary differential equation) instead of the algebraic equations (Equations 9.10 and 9.11), one equation is needed to model the inorganic sulfur dynamics and another equation is needed to model either H_2S or HS^- (Batstone *et al.*, 2002; Jeppsson & Rosen, 2006). The other compound is calculated as the total inorganic sulfur minus the calculated compound (e.g. $S_{h2s} = S_{IS} - S_{hs-}$). When utilizing ODE, all chemical species are included in the state vector and thus stoichiometry and kinetics are defined in terms of species (Lizarralde *et al.*, 2015). This modification also requires the inclusion of an additional rate equation for the acid-base reaction (Equation 9.14), where $\rho_{A/B,h2s}$ is the product rate of H_2S from HS^- (i.e. base to acid) and $k_{A/B,h2s}$ is the acid-base kinetic parameter ($1 \times 10^{10}\ M^{-1} \cdot day^{-1}$) (Jeppsson & Rosen, 2006):

$$\rho_{\underset{B}{A},h2S} = k_{\underset{B}{A},h2S} \cdot (S_{hs-}(S_{h+} - K_{a1}) - K_{a1}S_{IS}) \tag{9.14}$$

9.2.1.5 Gas-liquid H_2S mass-transfer

To calculate the concentration of H_2S in the biogas and in the liquid phase, it is necessary to consider the H_2S mass-transfer between the liquid and the gas phase. Henry's law, which expresses the concentration in the liquid phase due to a gas partial pressure, has been used to describe the equilibrium between both the liquid and the gas phase (Cassidy *et al.*, 2015; Kalyuzhnyi *et al.*, 1998). Equation 9.15 is the single-film mass-transfer equation to dynamically model the exchange of H_2S between both phases:

$$\rho_{T,h2S} = k_L a \cdot (S_{h2s} - 64 \cdot K_{H,h2s} \cdot p_{h2S,gas}) \tag{9.15}$$

where $\rho_{T,h2S}$ is the specific mass-transfer rate of H_2S from the liquid to the gas phase, $k_L a$ is the gas-liquid transfer coefficient (200 day^{-1}, as most common default value although highly variable depending on mixing, temperature, etc.), S_{h2s} is the hydrogen sulfide concentration in the liquid phase, $K_{H,h2s}$ is the Henry's law coefficient for H_2S ($0.001\ M \cdot bar^{-1}$ (Batstone *et al.*, 2002)), 64 is a conversion factor to convert the Henry's law coefficient from molar to chemical oxygen demand (COD) basis, and $p_{h2s,gas}$ is the partial pressure of H_2S in the headspace (bar). The impact of temperature on the Henry's law coefficient should be also considered in the model (Majer *et al.*, 2008).

9.2.1.6 Metal precipitation

Metal precipitation modeling has received less attention than the physical and biochemical reactions, likely due to the difficulty in implementing and validating the model as well as the inexistence of a standardized model structure. However, metal precipitation is important since (i) sulfate reduction technology is used to produce H_2S which in turn is used to remove/recover metals as metal sulfide

precipitates, and (ii) ferrous and ferric chloride are used to precipitate sulfides in anaerobic digesters (Hussain *et al.*, 2016; Kaksonen & Puhakka, 2007; Lewis, 2010).

There are two main methods to model chemical precipitation in anaerobic biotechnologies: (i) an equilibrium-based model solved using algebraic equations, and (ii) a kinetic-based model solved using ODE. The equilibrium-based model assumes that precipitation reactions are fast and, therefore, there is enough reaction time for ions to form the precipitates and reach equilibrium (Barat *et al.*, 2013; Lewis *et al.*, 2003; Lizarralde *et al.*, 2015). The equilibrium-based model precipitates the ions present in a supersaturated solution based on the minerals solubility product constant (K_{sp}) values until the equilibrium is reached. Gupta *et al.* (1994) used an equilibrium-based model to simulate metal sulfide and carbonate precipitation. The main advantages of an equilibrium-based model are the lower computational demand and the fact that it relies on well-known electrolyte solution thermodynamics (Kazadi Mbamba, 2016). However, in these models, the precipitate with the lowest K_{sp} prevails over other mineral phases. On the other hand, the kinetic-based precipitation model allows control of the rate at which the precipitation reaction progresses towards the equilibrium. Therefore, at the end of an integration step the aqueous solution may still be supersaturated or undersaturated (Kazadi Mbamba, 2016). Note that if the precipitation rate is fast enough, the kinetic-based and the equilibrium-based models should achieve identical results. Nonetheless, since there is no standardized model, there are several kinetic-based precipitation models available in the literature utilizing different structures and equations (Barat *et al.*, 2013; Kazadi Mbamba *et al.*, 2015; Kralj *et al.*, 1997; Lewis, 2010; Lizarralde *et al.*, 2015).

A pioneering approach towards a kinetic-based precipitation model for precipitation in wastewater streams was developed for the Activated Sludge Model No. 2d (ASM2d) by Henze *et al.* (1999). In the ASM2d model, iron phosphate ($FePO_4$) precipitation and redissolution were modeled using Equations 9.16 and 9.17, where iron phosphate (X_{FePO4}) precipitates from the reaction between phosphate (S_{PO4}) and ferric hydroxide ($X_{Fe(OH)3}$):

$$\rho_{pre,FePO_4} = k_{cryst,FePO4} \cdot S_{PO_4} \cdot X_{Fe(OH)_3} \tag{9.16}$$

$$\rho_{red,FePO_4} = k_{diss,FePO4} \cdot X_{FePO_4} \tag{9.17}$$

In Equation 9.16 and 9.17, $k_{cryst,FePO4}$ is the iron phosphate precipitation rate, and $k_{diss,FePO4}$ is the iron phosphate redissolution rate. The main limitation of the ADM2d precipitation model is that it does not approach equilibrium conditions, since precipitation occurs because soluble phosphate and iron hydroxide are present in the reaction media (Kazadi Mbamba, 2016). A much more comprehensive precipitation model was proposed by Koutsoukos *et al.* (1980) (Equation 9.18), which was later on modified by Musvoto *et al.* (2000), Barat *et al.* (2013) and Lizarralde *et al.* (2015). Although none of these studies included

metal sulfides precipitation, the proposed model is a generic model that can be easily adapted to model different mineral precipitations.

$$\rho_{\text{pre,MA}} = k_{\text{cryst,MA}} \cdot s \cdot \left[([M^{\text{m+}}]^{\upsilon+}[A^{\text{a-}}]^{\upsilon-})^{\frac{1}{\upsilon}} - ([M^{\text{m+}}]_0^{\upsilon+}[A^{\text{a-}}]_0^{\upsilon-})^{\frac{1}{\upsilon}} \right]^n \quad (9.18)$$

where $[M^{\text{m+}}]$, $[A^{\text{a-}}]$ and $[M^{\text{m+}}]_0$, $[A^{\text{a-}}]_0$ are the concentrations of the ions in solution at a given time and at equilibrium, respectively. $k_{\text{cryst,MA}}$ is the apparent precipitation rate constant of MA, s is a factor proportional to the number of growth sites available, υ^+ is the number of cations involved in the reaction, υ^- is the number of anions involved, and $\upsilon = \upsilon^+ + \upsilon^-$. The exponent n is a number determined experimentally and is equal to 2 for most precipitation reactions. Note that the product between $[M^{\text{m+}}]_0{}^{\upsilon+}$ and $[A^{\text{a-}}]_0{}^{\upsilon-}$ equals the solubility product of the mineral ($K_{\text{sp,MA}}$). Musvoto *et al.* (2000) suggested that, when no seed material is added, the precipitation rate ($k_{\text{cryst,MA}}$) and the growth site factor (s) could be combined in a single precipitation rate constant ($k_{T,\text{cryst,MA}}$). Barat *et al.* (2013) included a function based on the saturation index in the kinetic expressions related to the precipitation and dissolution processes, accounting therefore for undersaturated and oversaturated operating conditions. Lizarralde *et al.* (2015) expanded the model by including three different Monod-style functions to model the development of the supersaturation of a solution, the nucleation process, and the growth of the precipitates.

An alternative approach to model mineral precipitation is the one described in Kazadi Mbamba *et al.* (2015b, 2015a). The authors propose a semi-empirical first-order kinetic precipitation model in which precipitation rate depends on the concentration of a mineral in the aqueous solution (Equation 9.19). Non-zero seed experimental conditions were used ($X_{\text{MA,0}} = 1 \times 10^{-6}$ M). The model also includes a relative supersaturation term (σ), representing the magnitude of the driving force for precipitation, i.e. how far the aqueous solution is from equilibrium (Equation 9.20). As for Koutsoukos *et al.* (1980), the exponent n is the order of the precipitation reaction with respect to supersaturation. In Kazadi Mbamba *et al.* (2015b, 2015a), the exponent n was 2 for all minerals, except for struvite where n was 3.

$$\rho_{\text{pre,MA}} = k_{\text{cryst,MA}} \cdot X_{\text{MA}} \cdot \sigma^n \quad (9.19)$$

$$\sigma = \left(\frac{[M^{\text{m+}}]^{\upsilon+}[A^{\text{a-}}]^{\upsilon-}}{K_{\text{sp}}} \right)^{\frac{1}{\upsilon}} - 1 \quad (9.20)$$

The Kazadi Mbamba *et al.* (2015b, 2015a) model was implemented in the ADM1 by Flores-Alsina *et al.* (2016), who successfully modeled multiple mineral precipitation reactions, including iron sulfide precipitation in anaerobic digesters. It is important to highlight that Flores-Alsina *et al.* (2016) considered non-ideality, including ion complexation/pairing and ion activities instead of

molar ion concentrations. Knobel and Lewis (2002) also considered that the aqueous phase is a non-ideal solution. Indeed, few authors have considered non-ideality in their calculations, which represents a source of inaccuracy (Capson-Tojo *et al.*, 2020; Patón *et al.*, 2018; Solon *et al.*, 2015).

9.2.2 Models at biofilm level

Biological sulfate reduction in high-rate granular bioreactors has been largely researched at lab-scale (Hao *et al.*, 2014; Liamleam & Annachhatre, 2007). High-rate bioreactors are also the main bioreactor configuration in the full-scale sulfate reduction technologies by Paques BV, e.g. Thioteq™ and Sulfateq™ (Hedrich *et al.*, 2018; Huisman *et al.*, 2006). The main advantage of granular bioreactors (e.g. UASB and expanded granular sludge bed (EGSB)) is the superior capacity to retain microorganisms in the system than flocculent bioreactors (e.g. CSTR and plug flow), which allows improvement of the system efficiency and reduction of the reactor volume (Hao *et al.*, 2014; van Lier *et al.*, 2015). Additionally, the granule structure provides layered microenvironments and niches for the different microorganisms involved in the process (Feldman *et al.*, 2019; Hao *et al.*, 2014; Sun *et al.*, 2016). Biofilm modeling enables better understanding of the mass transport of substrates and their microbial conversion in the biofilm as well as the dynamics of the microbial community.

The main difference between suspended biomass models (see Section 9.2.1) and biofilm models is that biofilm models need to include additional terms to model the diffusion of the reactants and products within the biofilm. For that purpose, biofilm models have used Fick's second law in spherical coordinates (Equation 9.21), which allows modeling of the diffusion of the compounds in the biofilm under unsteady-state conditions, i.e. the model is able to model changes of concentration gradient over time (Devinny & Ramesh, 2005; Sun *et al.*, 2016). Considering that the diffusion is axisymmetric, the equation is typically simplified to Equation 9.22:

$$\frac{\partial S_i}{\partial r} = \frac{D_f}{r^2}\left(\frac{\partial}{\partial r}\left(r^2\frac{\partial S_i}{\partial r}\right) + \frac{1}{\sin\theta}\frac{\partial}{\partial\theta}\left(\sin\theta\frac{\partial S_i}{\partial\theta}\right) + \frac{1}{\sin^2\theta}\left(\frac{\partial^2 S_i}{\partial^2\phi}\right)\right) \tag{9.21}$$

$$\frac{\partial S_i}{\partial r} = D_f\left(\frac{\partial^2 S_i}{\partial^2 r}\right) \tag{9.22}$$

The diffusion coefficients in the biofilm need to be estimated or fitted using experimental data. Molecular diffusion constants for water are available for most compounds. However, diffusion coefficients within a biofilm may differ since the presence of microorganisms restricts the diffusion of compounds (Devinny & Ramesh, 2005). Fan *et al.* (1990) published an empirical formula that relates the diffusion coefficient measured in water with the one in the biofilm considering the biomass density in the biofilm. However, many other equations to estimate biofilm diffusion coefficients are available in the literature (Stewart, 1998).

A simpler approach was used by Sun *et al.* (2016), who set the diffusivity coefficients of the different compounds at 0.8-fold of the values in water.

Noguera *et al.* (1999) developed a mathematical model able to simulate the three-dimensional growth of two species in an anaerobic biofilm (i.e. SRB *Desulfovibrio vulgaris* and the methanogenic *Methanobacterium formicicum*), which used the kinetic and thermodynamic mechanisms developed in their previous publication (Noguera *et al.*, 1998). The model was able to predict different biofilm structures in the presence and in the absence of sulfate as well as when both microorganisms co-existed. The research by Noguera *et al.* (1999, 1998) complemented the theoretical study conducted by Overmeire *et al.* (1994), who showed the importance of sulfate mass transfer as a factor to comprehend the competition between sulfate reducers and methanogens in the anaerobic granules. The results of Overmeire *et al.* (1994) showed that sulfate reduction can be limited in UASB reactors by the sulfate mass transfer. However, the model did not include the competition between SRB and methanogens for the electron donor, nor the utilization of SRB products by methanogens (i.e. acetate from the incomplete oxidation of the carbon source). The model used by Overmeire *et al.* (1994) was a second-order differential (Equation 9.22) one, with one boundary condition for the center of the granule ($r = 0$, Equation 9.23) and one boundary condition for the granule interface ($r = R$, Equation 9.24):

$$\frac{1}{r^2}\frac{\partial}{\partial r}\left(D_f \cdot r^2 \frac{\partial S_{g,\mathrm{SO4}}}{\partial r}\right) = k_{m,\mathrm{SRB}} \frac{S_{g,\mathrm{SO4}}}{K_{S,\mathrm{SRB}} + S_{g,\mathrm{SO4}}} X_{\mathrm{SRB}} \tag{9.22}$$

$$\frac{\partial S_{g,\mathrm{SO4}}}{\partial r} = 0 \tag{9.23}$$

$$D_f\left(\frac{\partial S_{g,\mathrm{SO4}}}{\partial r}\right) = k_1 \cdot (S_{\mathrm{aq,SO4}} - S_{g,\mathrm{SO4}}) \tag{9.24}$$

where D_f is the diffusion coefficient of sulfate in the biofilm, $S_{g,\mathrm{SO4}}$ is the sulfate concentration in the granule, $k_{m,\mathrm{SRB}}$ is the maximum uptake rate of sulfate, $K_{S,\mathrm{SRB}}$ is the sulfate half-saturation constant, X_{SRB} is the SRB concentration in the granules, R is the radius of the granule, $S_{\mathrm{aq,SO4}}$ is the sulfate concentration in the liquid, and k_1 is the mass transport coefficient of sulfate in the stagnant liquid film between the liquid bulk and the granule surface.

The biological, chemical, and physical processes occurring in a methanogenic and sulfate-reducing granular reactor under dynamic conditions have been modeled by D'Acunto *et al.* (2011) and by Sun *et al.* (2016). D'Acunto *et al.* (2011) developed a convection-diffusion model, where a convection term controlled the biofilm growth and a diffusion term controlled the substrate and product gradients within the biofilm. The model included three distinct microbial groups (i.e. complete oxidizing SRB, incomplete oxidizing SRB, and methanogens) and three reactions (one reaction for each microbial group).

D'Acunto *et al.* (2011) predicted that SRB dominate the outmost layer of the granule while methanogens dominate the inner layers of the granule. D'Acunto *et al.* (2011) also found that the methanogenic layer gains dominance in the granule as the influent BOD:SO_4^{2-} ratio decreases. The microbial distribution obtained by D'Acunto *et al.* (2011) within the granule is in agreement with the one obtained by Sun *et al.* (2016). Sun *et al.* (2016) showed that SRB and fermentative bacteria dominate in the granule outer layer, while methanogens dominate in the granule inner layer. In Sun *et al.* (2016), a mathematical model based on growth kinetics of microorganisms and substrate transportation through biofilms was developed to describe methane production and sulfate reduction with ethanol as the key electron donor. The model was calibrated and validated using experimental data from two case studies conducted in a UASB reactor. The developed model could satisfactorily describe methane and sulfide production as well as ethanol and sulfate removal in both systems. The model outputs revealed a stratified distribution of methanogenic archaea, sulfate-reducing bacteria and fermentative bacteria in the anaerobic granular sludge and the relative abundances of these microorganisms vary with substrate concentration. It also revealed that sulfate-reducing bacteria outcompeted fermentative bacteria for ethanol utilization when the COD/SO_4^{2-} ratio was equal to or above 0.5. Model simulations suggested an optimal granule size for efficient methane production, while the sulfate reduction was not significantly affected by variation in granule size. Sun *et al.* (2016) also provided comprehensive insights by revealing that the methane production and sulfate reduction were affected by ethanol and sulfate loading rates as well as by the development stage of the microbial community. The model of Sun *et al.* (2016) was based on ADM1 and included six microbial groups, i.e. ethanol fermenters, ethanol-degraders SRB, acetate-degraders SRB, autotrophic SRB, acetoclastic methanogens, and hydrogenotrophic methanogens. Most importantly, Sun *et al.* (2016) were able to properly describe the methane production and sulfate reduction of a UASB reactor operated for over 180 days.

9.3 ON-LINE MONITORING

9.3.1 Sensors for sulfurous compounds

Different off-line techniques based on analytical measurements can be applied for monitoring AD processes due to their great reproducibility and precision. These techniques are, however, time consuming and require extensive manual handling. Thus, the choice of appropriate on-line monitoring techniques is crucial for efficiently controlling biological processes of this type, which are complex – due to their strong non-linearity and non-stationarity – and thus very difficult to control. For instance, a simple method for the determination of dissolved sulfide in colored complex media was developed at the end of the 1990s by Percheron *et al.* (1996) using ion exchange chromatography. Its principle was based on the complete oxidation of sulfide into sulfate through the strong oxidant hydrogen

peroxide. The difference in sulfate concentration gives the total dissolved sulfide concentration. Sulfide from continuous and discontinuous digestion of sulfate-rich wastewater has been successfully assayed by this technique. However, autoxidation and stripping of H_2S must be avoided, thus basification, refrigeration and/or other handling actions must be performed immediately after sampling, without bacterial separation.

On-line monitoring remains the weakest part of real-time AD systems process control. Accordingly, adequate selection of monitoring equipment is required to achieve accurate actions. Among the available sensors, the choice of a measurement device to be used for on-line control depends on several factors, such as its sensitivity to variations and its response time to a disturbance. Additional criteria should also be considered at the industrial scale such as low cost and low maintenance. For example, Jimenez *et al.* (2015) and Wu *et al.* (2019) presented comprehensive overviews of different monitoring techniques used in AD processes. Moreover, a comprehensive overview of real-time monitoring techniques to measure sulfide, electron donors, sulfate, and biomass composition can be found in Cassidy *et al.* (2015).

Within the anaerobic treatment of sulfate-rich wastewaters, sensors to probe sulfurous compounds are of the greatest importance. Classical on-line and off-line sulfide concentration measurements based on sensors consist of using an ion selective electrode (Bandekar *et al.*, 1995), a redox electrode (Janssen *et al.*, 1998), a titrimetric method (Zancato *et al.*, 1990), or a spectrophotometric method (Bandekar *et al.*, 1995). Nonetheless, the most widely implemented monitoring method to indirectly measure the overall activity of the process consists of analyzing the output gas composition and flow rate.

Different techniques are available for measuring the composition of the biogas including H_2S, such as Infrared (IR), Fourier transform infrared (FTIR), non-dispersive infrared (NDIR), ultraviolet (UV) and ultraviolet-visible (UV/VIS) photometers; diode laser sensing, specific analyzers based on electrochemical cells, thermal conductivity analyzers, and moisture sensors (Jimenez *et al.*, 2015; Redondo *et al.*, 2008; Wu *et al.*, 2019). From these on-line measurements, a soft sensor (also known as a virtual sensor) based on a theoretical evaluation from the Henry's law and the sulfide dissociation equilibrium can be used to calculate the concentration of dissolved compounds. Figure 9.3 shows a general

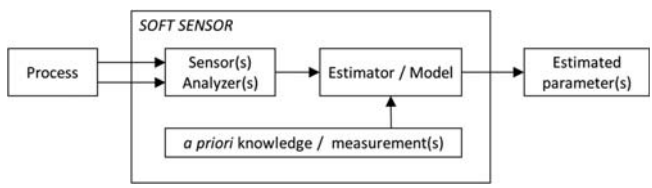

Figure 9.3 Schematic view of a soft sensor.

representation of a soft sensor, which can be defined as a numerical algorithm that combines signals from available hardware sensors within a given mathematical framework. They estimate an unknown parameter, taking advantage of the *a priori* knowledge available about a process (Bastin & Dochain, 1990).

9.3.2 In-situ sulfate sensors

Different electrodes can be used for sulfate monitoring, such as ion-selective electrodes (ISEs), which are usually chosen for routine applications since they have many advantages over other methods for anion concentration determination. Different sulfate-selective compounds were proposed at the end of the 1990s based on the Nernst potential for sulfate determination in liquid streams (see e.g. Berrocal *et al.*, 2000; Li *et al.*, 1999; Nishizawa *et al.*, 1998; Shamsipur *et al.*, 2001). The selectivity of an ISE towards sulfate is of great importance and must be taken into account when choosing an appropriate ISE sensor. The response of an ISE should, in theory, be in accordance with the Nernst equation (Cassidy *et al.*, 2015):

$$E = A - 2.303\frac{R \cdot T}{z_i \cdot F} \cdot \log(a_i) \tag{9.25}$$

where E is the electrode potential, A is a constant, R is the universal gas constant, T is the temperature, F is the Faraday constant, z_i is the ionic charge, and a_i is the activity of the ion.

Morigi *et al.* (2001) presented a sulfate-ISE based on a dispersion of hydrotalcite particles into a polymeric membrane using coated-wire (CW) configuration, testing membranes based on polyvinyl chloride (PVC) and polydimethylsiloxane (PDMS). Morigi *et al.* (2001) observed that both membranes exhibited strong and selective interactions with sulfate, despite better performances being obtained when using PDMS rather than PVC, with response times below 60 seconds, while the potentiometric response was practically constant in the pH range 4–7. Ganjali *et al.* (2002) presented a novel sulfate ion-selective polymeric membrane electrode based on a derivative of pyrilium perchlorate. This ISE showed good selectivity for the sulfate ion with respect to common organic and inorganic anions, exhibiting good linear responses within a pH range of 4–9. Another sulfate-selective PVC-based ISE was tested by Mazloum-Ardakani *et al.* (2012). These authors investigated the performance of this electrode using potentiometric and electrochemical impedance spectroscopy (EIS). The results showed that the prepared electrode had a detection limit of 6.3×10^{-7} M and a response time of less than 15 s.

Nezamzadeh-Ejhieh and Esmaeilian (2012) proposed a sulfate-ISE based on surfactant-modified zeolite particles into carbon paste. The electrode exhibited a linear response range to sulfate species in the range of 10^{-6} to 10^{-3} M with a detection limit of 2×10^{-6} M and a good sensitivity based on the Nernstian slope

within the pH range 4–10. Lomako *et al.* (2006) also evaluated a sulfate-ISE based on the composition of a neutral carrier and a quaternary ammonium salt. The ISE was used for the determination of sulfate in seawater, mineral water and urine by a direct potentiometric method and potentiometric titration, resulting in relative errors below 7%. Mazloum-Ardakani *et al.* (2006) presented a sulfate-ISE based on a complex of copper as a membrane carrier. The electrode exhibited good sensitivity and linearity within the range of 10^{-7}–10^{-1} M. The probe resulted in a fast response time of 10 seconds and had a lifetime of more than three months within the pH range 3.5–8.0. Fibbioli *et al.* (2000) investigated a polymeric membrane ISE based on an anionic chloro-borane cluster and a dihydrochloride analogue for phosphate and sulfate monitoring. The best sulfate selectivity was found for ISE membranes based on the dihydrochloride, whereas those with the zwitterion analogue were shown to possess a reasonably good selectivity for monohydrogen phosphate. More recently, Gołębiewski *et al.* (2019) studied an electrochemical sensor comprising a cyclopeptide connected to the surface of a gold electrode via a bis(dipyrromethene) Cu(II) or Co(II) complex for the detection of sulfate in water. The sensor displayed high selectivity and sensitivity, rendering it potentially useful for environmental monitoring.

Although further research is needed to develop industrially-feasible ISEs, these solutions are of great interest for real-time controlling sulfate-rich processes. On-line dissolved sulfate measurements are very important when treating sulfate-rich wastewaters since the influent BOD:SO_4^{2-}-S ratio strongly affects the feasibility of AD systems due to the competition of SRB and methanogens for the available substrate. Thus, these ISE sensors would enable the development of control strategies aimed to optimize methane production or to minimize H_2S inhibition, among others.

9.3.3 In-situ sulfurous compounds sensors

Regarding H_2S, Pandey *et al.* (2012) broadly discussed the use of different sensors for H_2S measurement in the gas phase, such as the following:

- Semiconducting metal-oxide sensors in the form of thin or thick films, based on metal-oxide semiconductors (e.g. tin oxide). These sensors present a small size, simple construction, low weight, low power consumption, and low cost (Fine *et al.*, 2010). The heated metal-oxide sensor is the most commonly used sensor for monitoring gases.
- Electrochemical sensors based on liquid and solid electrolyte sensors, with solid electrolyte being the most commonly used electrochemical sensors for H_2S-gas analysis. Amperometric-based electrochemical sensors generate a current signal that is related to the H_2S concentration by Faraday's law and the laws of mass transport. Potentiometric-based electrochemical sensors measure electrical potential (voltage).

- Optical sensors use an optical sensing technique, based on the attenuation of light waves, commonly employing optical transduction techniques to yield H_2S information (McDonagh *et al.*, 2008). Optical chemical sensors can generally be categorized into two types, i.e. direct and reagent mediated. In direct sensing, H_2S is detected via its intrinsic optical property (e.g. absorption or luminescence). In reagent-mediated sensors, a change in the optical response of an intermediate agent is used for measurement. For instance, Cho *et al.* (2008) proposed a wireless electronic nose system for real-time quantitative analysis of gas mixtures using a gas sensor micro-array and neuro-fuzzy network, showing good performance in the concentration range of 0.15–1.5 ppm H_2S with a high sensibility and response time (0.2 s).
- Conducting-polymer sensors are widely used for gas characterization due to their easy fabrication (see e.g. Virji *et al.*, 2005), high reproducibility, rapid reaction rate, and low cost compared to other techniques. The basic idea is to mix conducting materials with polymers selected for the target gas to form a conducting-polymer-composite sensing material.
- Piezoelectric sensors are configured as mass-change-sensing devices. Generally, these devices are a resonating polymer-coated disk with metal electrodes, each side of which is connected to a lead wire. These sensors resonate at a characteristic frequency via excitation by a specific oscillating signal. Another type of piezoelectric device is the surface acoustic wave device, which is based on the principle that a Ray-Leigh wave travels over the surface of the device instead of through its volume (Tigli & Zaghloul, 2007).

On the other hand, on-line dissolved sulfide monitoring is also of great importance when treating sulfate-rich wastewaters. ISEs can also be used for this purpose. Moreover, from the measured activity of free sulfide ions with an ISE, the analytical concentration of the total dissolved sulfide (TDS) can be calculated if the protonation constants of the sulfide ion (K_1 and K_2) and the pH of the sample solution are known (Cassidy *et al.*, 2015), as shown in Equation 9.26, creating a virtual sensor based on ISE, pH and equilibrium calculations:

$$S^{2-} = \frac{\text{TDS}}{1 + \frac{H^+}{K_1} + \frac{(H^+)^2}{K_2}} \tag{9.26}$$

For instance, Grootscholten *et al.* (2008) designed an on-line estimator based on Equation 9.26 for the sulfide and zinc concentrations in a precipitation reactor. This virtual sensor allowed estimation of ZnS concentrations and precipitation rates in a CSTR based on the pH and the activity of the S^{2-} measured through an ISE. An appropriate performance was observed on the basis of experimental data, offering good possibilities for application in other metal removal processes.

Different sulfide-ISEs were developed in the 1980s and 1990s for sulfur determination in liquid (see e.g. Atta *et al.*, 1998; Guterman *et al.*, 1983; Tóth *et al.*, 1988) and even solid (García-Calzada *et al.*, 1999) samples. However, results on sulfide-ISEs seem to be less accurate than those obtained for sulfate-ISEs due to different inferences on the measuring principle. For instance, Balasubramanian and Pugalenthi (2000) critically analyzed ISEs and iodimetry for the determination of sulfide in tannery wastewater, showing significant deviations of ISEs from reference values. In this case, the accuracy of the values obtained through ISEs depended on the different effluent streams from which the samples were collected. Villa-Gomez *et al.* (2014) used a sulfide-ISE that was shown to be informative for applications in sulfate-reducing bioreactors and was successfully used for control purposes. However, the response of the probe showed a time-varying behavior due to sulfide accumulation or utilization of substrate sources that were not accounted for. Therefore, the recorded sulfide values needed to be corrected for pH variations and high sulfide concentrations ($>200\ mg \cdot L^{-1}$). On the other hand, Nezamzadeh-Ejhieh and Afshari (2012) modified a PVC-membrane electrode with the surfactant zeolite for potentiometric determination of sulfide, showing successful sulfide determinations in waste samples from a sugar company. This electrode exhibited a linear response range to sulfide in the range of 10^{-7} to $10^{-1}\ mol \cdot L^{-1}$ with good sensitivity to potential changes and a detection limit of $6.3 \times 10^{-8}\ mol \cdot L^{-1}$ within the pH range 3–10.

Regarding combined systems, Redondo *et al.* (2008) designed an automated H_2S on-line analyzer to assess the composition of the liquid and gas phases. The analyzer consisted of an Ag_2S ISE to detect S^{2-} in the liquid phase and a continuous flow analyzer with a gaseous diffusion step for detecting H_2S in the gas phase. High Nernstian slopes were achieved.

9.3.4 Biosensors

Cassidy *et al.* (2015) reviewed the possibilities of combining in-situ sensors with molecular techniques to get better insights into the processes prevailing in a bioreactor, such as combining microelectrodes with specific oligonucleotide probes (Ramsing *et al.*, 1993), or combining molecular techniques (DGGE: denaturing gradient gel electrophoresis, PCR: polymerase chain reaction and FISH: fluorescence in situ hybridization) with microsensors for H_2S and CH_4 (Santegoeds *et al.*, 1999). However, these techniques for biomass and activity characterization are invasive, destructive, expensive, and provide off-line data. Hence, further research is required to quantify microbial activity in real-time. In this respect, impedimetric biosensors would allow quantification of different biological-related processes, such as the following: monitoring microbial populations using an impedimetric immunosensor (Wan *et al.*, 2009), antibody recognition through direct immobilization on a bioinspired architecture as a sensing platform (Wan *et al.*, 2011), evaluation of redox indicators under

dechlorinating conditions (Jones & Ingle, 2005), amplification of responses of vancomycin-functionalized magnetic nanoparticles using a modified quartz crystal microbalance (Wan *et al.*, 2010a), potentiometric stripping analysis for the detection of *Desulforibrio caledoiensis* (Wan *et al.*, 2010b), or monitoring the treatment of acid mine drainage using conductivity (Lyew & Sheppard, 2001).

9.4 CONTROL

9.4.1 Process control in AD

AD must be optimized to enhance resource recovery with minimum energy input. However, AD optimization is not straightforward due to the inherent complexity involved in anaerobic processes. In particular, sensitivity to process overloads and other disturbances such as acidification, inhibition and toxicant exposure, rheology, foaming, stirring and mixing problems, as well as low/high C:N ratios (i.e. ammonia inhibition and lack of macro- and micro-nutrients) are among the main situations that can be faced in practice. These factors may lead to different operational problems including biomass washout. Over the years, research on AD has advanced, allowing for widening the application field of AD: from the side-stream treatment of sewage and biological sludge to the mainstream treatment of wastewater (industrial and municipal/urban), and to the (co-) digestion of the organic fraction of municipal solid waste, food waste or different kinds of agricultural residues. Therefore, control targets have also evolved, moving from the classical regulation of key variables to the prediction of overall AD process performance, including feeding optimization (e.g. blending of co-substrates).

AD is a mature technology that relies on a synergistic effort of a diverse group of microbial communities to metabolize diverse organic substrates (see Figure 9.1). However, AD is sensitive to process disturbances, and thus it is advantageous to use on-line monitoring and process control techniques to efficiently operate AD processes: Section 9.3 overviewed the range of electrochemical, chromatographic and spectroscopic devices that can be implemented for on-line AD monitoring and control. Complexity of the control strategy ranges from a feedback control to advanced control systems.

Different operating and control strategies have been proposed, from open-loop and off-line control approaches to advanced automatic (closed-loop) control systems. Several examples of control strategies applied to different AD systems can be found elsewhere, mostly using continuous in situ monitoring and associated feedback procedures to routinely deliver continuous and optimal performance (Gaida *et al.*, 2017; Jimenez *et al.*, 2015; Nguyen *et al.*, 2015; Olsson *et al.*, 2014; Robles *et al.*, 2018; Ward *et al.*, 2008). Over the last 40 years many different control methodologies for substrate feed control of AD processes have been developed to improve plant efficiency and sustainable long-term energy production (Gaida *et al.*, 2017). Regardless of the application, such control aims to find a compromise between maximizing economic yield,

minimizing the ecological footprint and minimizing the risk of process failure (Gaida *et al.*, 2017).

9.4.2 Advanced closed-loop control of AD processes

Besides classical proportional-integral-derivative (PID) control and derivatives (e.g. PI – proportional integral), different advanced control approaches have been applied to different AD processes, such as disturbance monitoring control, model predictive control, adaptive control, robust control, fuzzy control, artificial neural networks, and fault detection and isolation, among others. A summary of the main characteristics of these controllers is presented in this chapter.

9.4.2.1 Disturbance monitoring control

The control of wastewater treatment processes in general – and for the treatment of waters polluted by sulfurous compounds in particular – can be achieved through a careful analysis of the disturbances affecting the main variables. The purpose of the "disturbance monitoring" is to develop a control strategy that, compared to conventional controllers, tackles the problem of process overloading very differently (Steyer *et al.*, 1999). The basic idea of this control strategy is to add a disturbance on the input liquid flow rate. The response of simple parameters, that can be chosen because of their heavy use at the industrial scale (e.g. pH and the output gas flow rate), can be analyzed to determine if it is possible to increase the loading rate of the reactor. A negative effect of a positive disturbance (e.g. an increase of the input liquid flow rate) can be observed by a pH decrease or by an increase of the output gas flow rate lower than theoretically expected. In such a case, the reactor is assumed to be overloaded and the organic loading rate is automatically decreased. In the case of no negative effect of the disturbance, the reactor is assumed to operate safely (i.e. without being overloaded) and the loading rate is increased. Thus, the organic loading rate can be maintained as high as possible despite influent variability and the organic matter concentration of the treated effluent can be kept low and stable (Steyer *et al.*, 1999).

9.4.2.2 Model-based and linearizing control

The model-based control principle is largely used in the process industry. These controllers take advantage of available mathematical models for optimization purposes. Model-based control could allow efficient control of the running of a digester while achieving more precise actions than those controllers based on the difference between measurements and set points. For instance, linearizing control is based on the linearization of a non-linear system in order to achieve linear closed-loop dynamics. However, due to the strong non-linearity of AD processes, linearizing controllers only attain proper results when the process dynamics are bound by a defined linear zone. This kind of controller is built in a two-step procedure (Kurtz & Henson, 1997). Firstly, a non-linear model is used in order to

synthesize the non-linear state feedback controller that linearizes the map between a "new" manipulated input and the controlled output. In the second step, a linear pole placement controller is designed for the feedback linearized system.

9.4.2.3 Adaptive control

The key idea of an adaptive control design is to take advantage of the well-known parameters associated with the dynamics of bioprocesses (basically, the reaction pathways and mass balances summarized in a dynamic mass balance model) while accounting for the model uncertainty (mainly the kinetics). Since the model is generally non-linear, the model-based control design might result in a linearizing control structure, in which the on-line estimation of the unknown variables (concentration of pollutant and its intermediates) and parameters (reaction rates and yield coefficients) are incorporated.

Adaptive control schemes can be applied for AD processes because of their good disturbance rejection ability (Renard *et al.*, 1988). In such cases, the parameters of the controller are continuously adapted to follow – and sometimes to estimate – the changes in the operating conditions (Dochain & Perrier, 1993).

9.4.2.4 Robust control

One of the key issues to be addressed in controlling biological wastewater treatment processes is to reject the disturbances that can destabilize the reactor. It is worth mentioning that a clear distinction must be made between disturbance rejection and insensitivity to unmodeled phenomena or parameter variations. Robust control strategies represent a promising option to tackle these two problems since this control strategy includes significant improvements over conventional PID controllers (Flores-Estrella *et al.*, 2019; Méndez-Acosta *et al.*, 2010). Regarding adaptive control, robust control approaches strongly rely on mathematical models such as those depicted in Section 9.2. However, the main difference between robust and adaptive control schemes is that the latter continuously adapt their parameters based on dynamic estimates of the process evolution whereas, in the former scheme, the uncertainty is explicitly accounted for in the building of the controller. The adaptive control scheme can thus achieve a better performance whereas the robust control scheme can handle more severe operating conditions (Steyer *et al.*, 2006).

9.4.2.5 Fuzzy control

AD is a complex process which presents important challenges to be controlled with classic PID methods. However, this imperfect knowledge of the process can be minimized through expertise obtained with the operation of pilot units. Since fuzzy logic naturally captures the acquired experience of human operators, it appears to be a powerful tool for controlling this type of process (Driankov *et al.*, 1996; Zadeh, 1965). In addition, fuzzy logic can incorporate semi-quantitative

information into simplified models and it can put subjective information into a form usable by computers.

Fuzzy control allows efficient management of a wastewater treatment plant in general – and an AD process in particular (Estaben *et al.*, 1997). In addition, fuzzy logic has very interesting properties since human operators and/or control engineers generally find it difficult to decide upon adequate parameters to use when dealing with a full-scale wastewater treatment plant. The fuzzy control theory can be used to implement effective control strategies even when suitable models or correct parameters are unknown. Last but not least, this method can be extended to many different applications in the wastewater treatment field since a fuzzy controller can be easily tuned (Driankov *et al.*, 1996).

9.4.2.6 Artificial neural networks

Section 9.4.2 has so far outlined several difficulties which arise upon the implementation of control systems for wastewater treatment and the AD process. Firstly, the behavior of biological processes and the models describing these systems (see Section 9.2) are often highly non-linear. Additionally, these models are complex and their parameters are often difficult to determine. The dynamics of biological processes also tend to vary because of variations in metabolism and environmental parameters.

Application of artificial neural networks (ANNs) overcomes all these problems since ANNs can approximate any non-linear mapping arbitrarily and their learning abilities together with their parallel structure make them suitable for adaptive on-line application (Funahashi, 1989; Hornik *et al.*, 1989). It is thus clear that artificial neural networks are promising for the modeling and control of biological and AD processes (Premier *et al.*, 1999; Wilcox *et al.*, 1995).

9.4.3 Process control of sulfate-reducing bioprocesses

The number of closed-loop control applications in sulfate-reducing bioprocesses is still scarce. Nonetheless, there is a good number of open-loop strategies that may help to improve the performance of these systems. Moreover, mathematical models (see Section 9.2) may serve as support for the design of enhanced operating and control strategies when there are available monitoring techniques (see Section 9.3).

Many operating strategies have been used to control the conversion of sulfate into sulfide and the underlying problems related to corrosive sulfide formation (see Chapter 6). Sulfate-reducing process control has mainly focused on regulating the competition among microbial groups, optimizing the input ratio of electron donors to acceptors, and/or minimizing sulfide production. Specifically, the competition for the use of available substrates between SRB and methanogens strongly reduces the energy recovery from waste, especially in the case of treating wastewaters with low BOD:SO_4^{2-}-S ratios such as urban wastewater.

Moreover, the generated H_2S has a higher impact on methanogenic than on SRB activity (Chen *et al.*, 2008). However, the control of the influent sulfate concentration is generally considered as an unrealistic option (Cirne *et al.*, 2008; Jimenez *et al.*, 2015), thus control of sulfate-reducing processes has been generally focused on four main alternatives conceived to control the negative effects of sulfide: (i) prevent sulfide formation with the addition of SRB inhibitory compounds (e.g. molybdate, divalent transition metals, antibiotics); (ii) addition of small amounts of oxygen in the anaerobic digester to oxidize sulfide to sulfur or sulfate (microaeration); (iii) addition of organic and inorganic salts to precipitate sulfur; and (iv) biogas desulfurization in an external gas treatment unit (Cirne *et al.*, 2008; Jimenez *et al.*, 2015). Specifically, microaeration and salts addition for metal precipitation are two strategies that can be efficiently optimized through the implementation of an automated control system. Chemical technologies to mitigate H_2S inhibition (i.e. to oxidize the sulfide) include precipitation by addition of metal salts and addition of oxidizing reagents like chlorine, hydrogen peroxide, or potassium permanganate. Biological methods include biological oxidation of H_2S by sulfur-oxidizing bacteria and inhibition of SRB activity (Liu *et al.*, 2015).

9.4.3.1 Control of H_2S emissions

9.4.3.1.1 H_2S oxidation in bioreactor effluent

McFarland and Jewell (1989) presented one of the first studies dealing with control algorithms applied to AD processes treating sulfate-rich wastewaters. They recommended pH adjustment for biogas sulfide control under conditions in which the influent sulfur level is below sulfide inhibitory concentrations, showing that control of gaseous sulfide levels through insoluble iron (Fe^{3+}) phosphate addition is an efficient control strategy with no adverse effects on digester performance. Later, Camp and Sublette (1992) used another system – a PC-based machine vision system – to continuously monitor changes in biomass concentration and to control the undesirable production of colloidal elemental sulfur (a reactor upset condition due to an inhibitory sulfide concentration) in a bioreactor containing *Thiobacillus denitrificans*. A video camera was established which produced regions of different background lighting. Mean values of the distribution of red, green and blue intensity components with corresponding regions of a digital image captured from the camera were used to monitor color changes associated with changes in biomass concentration and to determine if the reactor was under suboptimal operational conditions. They showed that the ratio of red to blue intensity was an important parameter in detecting the formation of an elemental sulfur precipitant. Using a stepper motor-driven pressure regulator, process control was then performed by altering the hydrogen sulfide flow rate setpoint based on the vision system measurements. At the end of the 1990s, Janssen *et al.* (1998) showed that the formation of elemental sulfur from the biological

oxidation of sulfide could be optimized by controlling the redox state of the solution. They successfully applied a PI control of the redox potential so that nearly stoichiometric amounts of oxygen were supplied to the system. In this way, the supplied oxygen was sufficient for oxidizing sulfide to sulfur, although about 10% of the sulfide was still oxidized to sulfate.

9.4.3.1.2 H_2S oxidation in biogas

Microaeration is considered a highly efficient, simple, reliable, and economically feasible technique for removing hydrogen sulfide from biogas (Cirne *et al.*, 2008; Khoshnevisan *et al.*, 2017; Krayzelova *et al.*, 2015). During microaeration, the oxygen added to the anaerobic digester promotes sulfide oxidization to elemental sulfur through chemical oxidation or by the so-called sulfide-oxidizing bacteria (SOB). However, microaeration is commonly conducted as an open-loop strategy, and only a few automated applications are available. In any case, precise dosing of O_2 is required to maximize the efficiency of anaerobic digestion. The appropriate oxygen dosing depends on the microaeration target: preventing volatile fatty acids (VFA) accumulation or removing hydrogen sulfide (Nguyen & Khanal, 2018).

The optimization of the O_2:S^{2-} ratio or the dissolved oxygen (DO) concentration (i.e. working under oxygen limiting conditions: DO concentrations $<0.1\ mg \cdot L^{-1}$) enables elemental sulfur to be obtained as a main end-product, which is the most desirable option from an economic point of view (Janssen *et al.*, 1995). Besides, optimizing the amount of required oxygen for H_2S oxidation can lead to the potential recovery of elemental sulfur. Hydrogen sulfide removal efficiencies higher than 90% can be achieved with microaeration (Fdz.-Polanco *et al.*, 2009; Jenicek *et al.*, 2010; Ramos *et al.*, 2014). Another factor affecting the efficiency of microaeration that could be used as a manipulated variable in a closed-loop controller is the residence time of biogas in the headspace volume, especially when air is dosed into the headspace. Removal efficiencies close to 100% have been reported (Díaz *et al.*, 2011; Ramos & Fdz-Polanco, 2014) with biogas residence times over 5 hours. These high efficiencies are due to the fact that SOB usually grow on the walls of the headspace.

Different control parameters have been used for maintaining an appropriate oxygen injection rate in dynamic systems in order to cope with variations in hydrogen sulfide production. Ramos and Fdz-Polanco (2014) developed a PID controller to control the air flow rate according to the H_2S concentration in biogas. Other authors (Khanal & Huang, 2006; Nghiem *et al.*, 2014) modified the air dosing rate in order to maintain the set point established for the oxidation reduction potential (ORP). Microaeration operated at a constant dosing rate could indeed result in oxygen overdosing thus decreasing methane production (Kobayashi *et al.*, 2012). The strategy of intermittent microaeration has also been applied in different studies. Nguyen *et al.* (2019) avoided VFA accumulation by

means of an intermittent (every 24 h) ORP-controlled microaeration strategy (at ORP of −470 mV).

Nonetheless, there are different factors to take into account in order to adequately establish control boundaries in terms of maximum oxygen dose, such as:

- Oxygen toxicity to methanogens: although oxygen is a well-known inhibitor for the activity of methanogens, the majority of microaeration studies have not revealed a significant decrease in the methanogenic activity. According to different authors (Estrada-Vázquez *et al.*, 2003; Shen & Guiot, 1996), methanogens are protected by facultative anaerobic bacteria in both granular and suspended sludge.
- Explosion risks of methane/oxygen mixtures: the flammable range for oxygen/methane mixtures are 85–95% air and 5–15% methane by volume (Appels *et al.*, 2008). The oxygen required for hydrogen sulfide removal is very small and not close to this range. However, the explosion risk should always be considered.
- Partial oxidation of soluble organic matter: the oxygen dosing rate required for microaerobic H_2S removal (0.001–0.01 $\cdot$ kg $m^{-3} \cdot day^{-1}$) is three orders of magnitude lower than the organic loading rate (OLR, 1–10 kg COD $\cdot$ $m^{-3} \cdot day^{-1}$). Therefore, the amount of oxidized substrate can be considered negligible (Krayzelova *et al.*, 2014).
- Dilution of biogas by nitrogen from air: when air is used for microaeration, nitrogen can significantly reduce the percentage of methane in the biogas, making its use difficult in cogeneration units. Celis (2012) reported that the percentage of nitrogen in the biogas increased up to 20% when treating biogas with high H_2S concentrations (around 12,000 ppm). Pure oxygen could be used in such cases, however, it increases the operational costs.
- An innovative method of microaeration is the application of water electrolysis within UASB reactors so that O2 is produced directly at the anode in the reactor (Tartakovsky *et al.*, 2011). A feedback control of the applied voltage can be used to control the oxygen production rate.

Automatic process control of microaeration still remains a great challenge for its implementation in full-scale applications (Chen *et al.*, 2020). Mathematical models may serve as support for the design of control strategies when there are available monitoring techniques. In this respect, Pokorna-Krayzelova *et al.* (2017) proposed the model ADM1-S:O, an ADM1 extension including the processes related to sulfate reduction and sulfide oxidation to elemental sulfur.

9.4.3.2 Metal precipitation

9.4.3.2.1 Metal addition for H_2S control

Another open-loop strategy commonly conducted for H_2S control is metal addition. Nonetheless, few automated applications are yet available. Closed-loop control for

metal precipitation would allow optimization of the dose of metal to be used for precipitation, optimizing the economics of the process.

Metal addition can be conducted onsite or even in the sewer systems (Zhang *et al.*, 2008). For instance, Salehin *et al.* (2019) evaluated different alternatives for reducing coagulants usage in urban water management. Specifically, Salehin *et al.* (2019) revealed that iron dosed to sewers is still available for hydrogen sulfide removal from biogas in the downstream WWTP. This study, which was performed under real-life conditions, confirmed the practical feasibility and effectiveness of the strategy through a year-long full-scale investigation. Regarding metal addition in AD systems, Lee *et al.* (2016) evaluated the effects of $FeCl_3$ addition on the operation of a staged anaerobic fluidized membrane bioreactor (SAF-MBR). Total sulfur removal increased to 87–95% with $FeCl_3$ addition. Sulfide removal increased to 90% with addition of $FeCl_3$ at the molar Fe^{3+}:S ratio of 0.54 and to 95% when the ratio was increased to 0.95. The effluent sulfide concentration also decreased to 0.3–0.6 mg $\cdot$ L^{-1} after the addition of $FeCl_3$. However, the addition of $FeCl_3$ negatively affected membrane fouling of anaerobic membrane bioreactors (AnMBR) due to the precipitation of inorganic foulants on the membrane surface. Other actions related to direct metal addition have been carried out for controlling H_2S production in AD systems. These actions reveal the potential of automated control of metal addition in order to minimize H_2S emissions. However, other factors such as phosphorus precipitation with metal and pH affecting H_2S dissociation must be also considered when developing control systems.

Nonetheless, not all metals are useful for potential automated control applications. For example, Akgul *et al.* (2017) assessed the effect of iron and aluminum-based coagulants on the formation of volatile sulfur compounds. Aluminum-based coagulants significantly increased volatile sulfur compound levels, while ferric chloride achieved up to 93% reduction of the biogas H_2S concentration.

The sulfide interaction with iron as regulator of the microbial community in AD systems is another factor to consider when designing automated control systems based on metal addition (Shakeri Yekta *et al.*, 2017). In this regard, control boundaries based on the S:Fe molar ratio might be defined since this ratio maintains a direct relation with methane production. An increase in the S:Fe molar ratio from 0.3 to 0.5 did not alter the methane production, while S:Fe molar ratios above 0.5–1.0 resulted in the accumulation of acetate in the digester and a decline in daily methane production.

9.4.3.2.2 Sulfide addition for selective metal precipitation

Besides the addition of metals for sulfide control, sulfide addition can also be used for selective metal precipitation. Different examples can be found in the literature using different types of ISE and pH sensors aiming to control chemical sulfide addition in a precipitation reactor. Table 9.1 shows some examples of control strategies applied for metal precipitation using chemical and biogenic sulfide.

Table 9.1 Examples of control strategies for metal precipitation from chemical and biogenic sulfide (extended from Cassidy *et al.*, 2015).

Controlled Variable	Manipulated Variable	Objective	Reference
Chemical sulfide concentration	Sulfide flow	Selective heavy metal precipitation (Cu-Zn and Pb-Zn)	Veeken *et al.* (2003)
Biogenic sulfide concentration	Sulfide flow	Zinc precipitation	König *et al.* (2006)
Biogenic sulfide concentration	Sulfide flow	Zinc precipitation	Esposito *et al.* (2006)
Chemical sulfide concentration	Sulfide flow	Copper and Zinc selective precipitation	Sampaio *et al.* (2009)
Chemical sulfide concentration	Sulfide flow	Zinc and Nickel selective precipitation	Sampaio *et al.* (2010)
Biogenic sulfide concentration	OLR	Sulfate reduction in a fluidized bed reactor	Villa-Gomez *et al.* (2014)

Veeken *et al.* (2003) proposed a process where a sulfide-selective ISE was used to control sulfide addition in order to remove heavy metals (Cd, Cu, Ni, Pb, and Zn). The heavy metals were removed to ppb levels at pH 6.0 by sulfide precipitation while maintaining the total sulfide concentration below 0.02 mg L^{-1}. By controlling the sulfide concentration at different levels, the metals in mixtures of Cu–Zn and Pb–Zn were selectively precipitated from solution, thus producing pure metal sulfide sludge that could be reused.

König *et al.* (2006) presented a dynamic model and a PI control strategy for the precipitation of ZnS. In this case, the sulfide concentration was also controlled using an ISE. The controller was able to handle sudden disturbances in the process conditions (pH, influent flow rate, or zinc and sulfide concentration). Esposito *et al.* (2006) also assessed the performance of a zinc sulfide precipitation process using a biogenic sulfide solution (the effluent of a sulfate-reducing bioreactor) as the sulfide source. A PI controller was used to control the pH and S^{2-} concentration at the desired level using a pH probe and a sulfide-selective ISE. Sampaio *et al.* (2009) evaluated the selective precipitation of Cu from Zn in a CSTR by using a sulfide-selective ISE. In this case, copper was continuously and selectively precipitated with Na_2S to concentrations below 0.3 ppb from water containing around 600 ppm of both Cu and Zn. Sampaio *et al.* (2010) studied the role of supersaturation within Zn–Ni sulfide selective precipitation. In this case, the selective removal of Zn with Na_2S from a mixture of Zn and Ni was studied in a CSTR operating at pH 5.

Villa-Gomez *et al.* (2014) evaluated progressive step changes in OLR to create sulfide responses for the design of a sulfide control in sulfate-reducing bioreactors. The sulfide was measured using a sulfide-selective ISE and the values obtained were used to calculate PID controller parameters. A rapid response and high sulfide increment were obtained through a stepwise increase in the influent COD concentration, while a stepwise decrease to the hydraulic retention time (HRT) resulted in a slower response with smaller sulfide increment. Regardless of the way that the OLR was decreased, the ISE response showed a time-varying behavior due to sulfide accumulation (HRT change) or utilization of substrate sources that were not accounted for (influent COD change). However, the ISE response was shown to be informative for application of substrate dosing in sulfate reducing bioreactors.

REFERENCES

Ahmed W. and Rodríguez J. (2018). Modelling sulfate reduction in anaerobic digestion: Complexity evaluation and parameter calibration. *Water Research*, **130**, 255–262.

Akgul D., Abbott T. and Eskicioglu C. (2017). Assessing iron and aluminum-based coagulants for odour and pathogen reductions in sludge digesters and enhanced digestate dewaterability. *Science of the Total Environment*, **598**, 881–888.

Arnell M., Astals S., Åmand L., Batstone D. J., Jensen P. D. and Jeppsson U. (2016). Modelling anaerobic co-digestion in Benchmark Simulation Model No. 2: Parameter estimation, substrate characterisation and plant-wide integration. *Water Research*, **98**, 138–146.

Angelidaki I., Treu L., Tsapekos P., Luo G., Campanaro S., Wenzel H. and Kougias P. G. (2018). Biogas upgrading and utilization: Current status and perspectives. *Biotechnology Advances*, **36**, 452–466.

Appels L., Baeyens J., Degrève J. and Dewil R. (2008). Principles and potential of the anaerobic digestion of waste-activated sludge. *Progress in Energy and Combustion Science*, **36**, 755–781.

Atta N. F., Galal A., Mark H. B., Yu T. and Bishop P. L. (1998). Conducting polymer ion sensor electrodes–III. Potentiometric sulfide ion selective electrode. *Talanta* **47**, 987–999.

Balasubramanian S. and Pugalenthi V. (2000). A comparative study of the determination of sulphide in tannery waste water by ion selective electrode (ISE) and iodimetry. *Water Research*, **34**, 4201–4206.

Bandekar, J., Sethna, R. and Kirshner, M. (1995). Quantitative determination of sulfur oxide species in white liquor bt FT-IR. *Applied Spectroscopy*, **49**(11), 1577–1582.

Barat R., Serralta J., Ruano M. V, Jiménez E., Ribes J., Seco A. and Ferrer J. (2013). Biological Nutrient Removal Model No. 2 (BNRM2): a general model for wastewater treatment plants. *Water Science and Technology*, **67**(7), 1481–1489.

Barrera E. L., Spanjers H., Dewulf J., Romero O. and Rosa E. (2013). The sulfur chain in biogas production from sulfate-rich liquid substrates: a review on dynamic modeling with vinasse as model substrate. *Journal of Chemical Technology and Biotechnology*, **88**, 1405–1420.

Barrera E. L., Spanjers H., Solon K., Amerlinck Y., Nopens I. and Dewulf J. (2015). Modeling the anaerobic digestion of cane-molasses vinasse: Extension of the Anaerobic Digestion Model No. 1 (ADM1) with sulfate reduction for a very high strength and sulfate rich wastewater. *Water Research*, **71**, 42–54.

Batstone D. J., Keller J., Angelidaki I., Kalyuzhnyi S. V., Pavlostathis S. G., Rozzi A., Sanders W. T. M., Siegrist H. and Vavilin V. A. (2002). The IWA Anaerobic Digestion Model No 1 (ADM1). *Water Science and Technology*, **45**(10), 65–73.

Batstone D. J., Keller J. and Steyer J. P. (2006). A review of ADM1 extensions, applications, and analysis: 2002–2005. *Water Science and Technology*, **54**(4), 1–10.

Batstone D. J., Puyol D., Flores-Alsina X. and Rodríguez J. (2015). Mathematical modelling of anaerobic digestion processes: applications and future needs. *Reviews in Environmental Science and Bio/Technology*, **14**, 595–613.

Bastin, G. and Dochain, D. (1990). On-line estimation and adaptive control of bioreactors, Elsevier Science Publishing, Amsterdam.

Berrocal M. J., Cruz A., Badr I. H. A. and Bachas L. G. (2000). Tripodal Ionophore with Sulfate Recognition Properties for Anion-Selective Electrodes. *Analytical Chemistry*, **72**, 5295–5299.

Camp C. E. and Sublette K. L. (1992). Control of a *Thiobacillus denitrificans* bioreactor using machine vision. *Biotechnology and Bioengineering*, **39**, 529–538.

Capson-Tojo G., Moscoviz R., Astals S., Robles Á. and Steyer J.-P. (2020). Unraveling the literature chaos around free ammonia inhibition in anaerobic digestion. *Renewable and Sustainable Energy Reviews*, **117**, 109487.

Cassidy J., Lubberding H. J., Esposito G., Keesman K. J. and Lens P. N. L. (2015). Automated biological sulphate reduction: A review on mathematical models, monitoring and bioprocess control. *FEMS Microbiology Reviews*, **39**, 823–853.

Celis C. A. (2012). Improvement of anaerobic digestion by using of microaerobic conditions. Department of Water Technology and Environmental Engineering, Ph.D., Institute of Chemical Technology in Prague, Prague, p. **181**.

Chen Y., Cheng J. J. and Creamer K. S. (2008). Inhibition of anaerobic digestion process: A review. *Bioresource Technology*, **99**, 4044–4064.

Chen Q., Wu W., Qi D., Ding Y. and Zhao Z. (2020). Review on microaeration-based anaerobic digestion: State of the art, challenges, and prospectives. *Science of the Total Environment*, **710**, 136388.

Cho J. H., Kim Y. W., Na K. J. and Jeon G. J. (2008). Wireless electronic nose system for real-time quantitative analysis of gas mixtures using micro-gas sensor array and neuro-fuzzy network. *Sensors Actuators B Chemical*, **134**, 104–111.

Cirne D. G., Van Der Zee F. P., Fernandez-Polanco M. and Fernandez-Polanco F. (2008). Control of sulphide during anaerobic treatment of S-containing wastewaters by adding limited amounts of oxygen or nitrate. *Reviews in Environmental Science and Biotechnology*, **7**, 93–105.

D'Acunto B., Esposito G., Frunzo L. and Pirozzi F. (2011). Dynamic modeling of sulfate reducing biofilms. *Computers & Mathematics with Applications*, **62**, 2601–2608.

Devinny J. S. and Ramesh J. (2005). A phenomenological review of biofilter models. *Chemical Engineering Journal*, **113**, 187–196.

Díaz I., Lopes A. C., Pérez S. I. and Fdz-Polanco M. (2011). Determination of the optimal rate for the microaerobic treatment of several H_2S concentrations in biogas from sludge digesters. *Water Science and Technology*, **64**(1), 233–238.

Dochain D. and Perrier M. (1993). Control Design for Nonlinear Wastewater Treatment Processes. *Water Science and Technology*, **28**(11–12), 283–293.

Driankov D., Hellendoorn H. and Reinfrank M. (1996). An Introduction to Fuzzy Control, 2nd edn. Springer-Verlag, Berlin, Heidelberg.

Durán F. (2013). Mathematical modelling of the anaerobic urban wastewater treatment including sulphate-reducing bacteria. Application to an anaerobic membrane bioreactor (Modelación matemática del tratamiento anaerobio de aguas residuales urbanas incluyendo las bacterias. Universitat Politècnica de València.

Durán F., Robles A., Seco A., Ferrer J., Ribes J. and Serralta J. (2017). Modelling the anaerobic treatment of urban wastewater: application to AnMBR technology. In: 15th IWA World Conference on Anaerobic Digestion (AD15), Beijing.

Esposito G., Veeken A., Weijma J. and Lens P. N.L. (2006). Use of biogenic sulfide for ZnS precipitation. *Separation and Purification Technology*, **51**, 31–39.

Estaben M., Polit M. and Steyer J. P. (1997). Fuzzy control for an anaerobic digester. *Control Engineering Practice*, **5**, 1303–1310.

Estrada-Vázquez C., Macarie H., Kato M. T., Rodríguez-Vázquez R., Esparza-García F. and Poggi-Varaldo H. M. (2003). The effect of the supplementation with a primary carbon source on the resistance to oxygen exposure of methanogenic sludge. *Water Science and Technology*, **48**(6), 119–124.

Fan L.-S., Leyva-Ramos R., Wisecarver K. D. and Zehner B. J. (1990). Diffusion of phenol through a biofilm grown on activated carbon particles in a draft-tube three-phase fluidized-bed bioreactor. *Biotechnology and Bioengineering*, **35**, 279–286.

Fdz.-Polanco M., Díaz I., Pérez S. I., Lopes A. C. and Fdz.-Polanco F. (2009). Hydrogen sulphide removal in the anaerobic digestion of sludge by micro-aerobic processes: pilot plant experience. *Water Science and Technology*, **60**(12), 3045–3050.

Fedorovich V., Lens P. and Kalyuzhnyi S. (2003). Extension of Enaerobic Digestion Model No. 1 with processes of sulfate reduction. *Applied Biochemistry and Biotechnology*, **109**, 33–45.

Feldman H., Flores-Alsina X., Ramin P., Kjellberg K., Jeppsson U., Batstone D. J. and Gernaey K. V (2019). Assessing the effects of intra-granule precipitation in a full-scale industrial anaerobic digester. *Water Science and Technology*, **79**(7), 1327–1337.

Fernández-Arévalo T., Lizarralde I., Fdz-Polanco F., Pérez-Elvira S. I., Garrido J. M., Puig S., Poch M., Grau P. and Ayesa E. (2017). Quantitative assessment of energy and resource recovery in wastewater treatment plants based on plant-wide simulations. *Water Research*, **118**, 272–288.

Fibbioli M., Berger M., Schmidtchen F. P. and Pretsch E. (2000). Polymeric Membrane Electrodes for Monohydrogen Phosphate and Sulfate. *Analytical Chemistry*, **72**, 156–160.

Fine G. F., Cavanagh L. M., Afonja A. and Binions R. (2010). Metal Oxide Semi-Conductor Gas Sensors in Environmental Monitoring. *Sensors* **10**, 5469–5502.

Flores-Alsina X., Solon K., Kazadi Mbamba C., Tait S., Gernaey K. V, Jeppsson U. and Batstone D. J. (2016). Modelling phosphorus (P), sulfur (S) and iron (Fe) interactions for dynamic simulations of anaerobic digestion processes. *Water Research*, **95**, 370–382.

Flores-Estrella R. A., Alcaraz-González V., García-Sandoval J. P. and González-Álvarez V. (2019). Robust output disturbance rejection control for anaerobic digestion processes. *Journal of Process Control*, **75**, 15–23.

Fomichev A. O. and Vavilin V. A. (1997). The reduced model of self-oscillating dynamics in an anaerobic system with sulfate-reduction. *Ecological Modelling*, **95**, 133–144.

Frunzo L., Esposito G., Pirozzi F. and Lens P. (2012). Dynamic mathematical modeling of sulfate reducing gas-lift reactors. *Process Biochemistry*, **47**, 2172–2181.

Funahashi K.-I. (1989). On the approximate realization of continuous mappings by neural networks. *Neural Networks*, **2**, 183–192.

Gaida D., Wolf C. and Bongards M. (2017). Feed control of anaerobic digestion processes for renewable energy production: A review. *Renewable and Sustainable Energy Reviews*, **68**, 869–875.

Ganjali M. R., Naji L., Poursaberi T., Taghizadeh M., Pirelahi H., Yousefi M., Yeganeh-Faal A. and Shamsipur M. (2002). Novel sulfate ion-selective polymeric membrane electrode based on a derivative of pyrilium perchlorate. *Talanta*, **58**, 359–366.

García-Calzada M., Marbán G. and Fuertes A. B. (1999). Potentiometric determination of sulphur in solid samples with a sulphide selective electrode. *Analytica Chimica Acta*, **380**, 39–45.

Gołębiewski P., Puciłowski B., Sommer F., Kubik S., Daniels M., Dehaen W., Sivasankaran U., Kumar K. G., Radecka H. and Radecki J. (2019). Electrochemical sensing of sulfate in aqueous solution with a cyclopeptide-dipyrromethene-Cu(II) or Co(II) complex attached to a gold electrode. *Sensors Actuators B Chemical*, **285**, 536–545.

Grootscholten T., Keesman K. and Lens P. (2008). Modelling and on-line estimation of zinc sulphide precipitation in a continuously stirred tank reactor. *Separation and Purification Technology*, **63**, 654–660.

Gupta A., Flora J. R.V., Sayles G. D. and Suidan M. T. (1994). Methanogenesis and sulfate reduction in chemostats—II. Model development and verification. *Water Research*, **28**, 795–803.

Guterman H., Ben-Yaakov S. and Abeliovich A. (1983). Determination of total dissolved sulfide in the pH range 7.5 to 11.5 by ion selective electrodes. *Analytical Chemistry*, **55**, 1731–1734.

Hao T., Xiang P., Mackey H. R., Chi K., Lu H., Chui H., van Loosdrecht M. C. M. and Chen G.-H. (2014). A review of biological sulfate conversions in wastewater treatment. *Water Research*, **65**, 1–21.

Harerimana C., Keffala C., Jupsin H. and Vasel J.-L. (2013). Development of a simple model for anaerobic digestion based on preliminary measurements of the bacterial sulphur activity in wastewater stabilization ponds. *Environmental Technology*, **34**, 2213–2220.

Hedrich S., Kermer R., Aubel T., Martin M., Schippers A., Johnson D. B. and Janneck E. (2018). Implementation of biological and chemical techniques to recover metals from copper-rich leach solutions. *Hydrometallurgy* **179**, 274–281.

Henze M., Gujer W., Mino T., Matsuo T., Wentzel M. C., Marais G. V. R. and Van Loosdrecht M. C. M. (1999). Activated sludge model No.2D, ASM2D. *Water Science and Technology*, **39**(1), 165–182.

Henze M., Gujer W., Mino T. and van Loosedrecht M. (2006). Activated Sludge Models ASM1, ASM2, ASM2d and ASM3. IWA Publishing.

Hornik K., Stinchcombe M. and White H. (1989). Multilayer feedforward networks are universal approximators. *Neural Networks*, **2**, 359–366.

Hughes M. N., Centelles M. N. and Moore K. P. (2009). Making and working with hydrogen sulfide: The chemistry and generation of hydrogen sulfide in vitro and its measurement in vivo: A review. *Free Radical Biology & Medicine*, **47**, 1346–1353.

Huisman J., Schouten G. and Schultz C. (2006). Biologically produced sulphide for purification of process streams, effluent treatment and recovery of metals in the metal and mining industry. *Hydrometallurgy*, **83**, 106–113.

Hussain A., Hasan A., Javid A. and Qazi J. I. (2016). Exploited application of sulfate-reducing bacteria for concomitant treatment of metallic and non-metallic wastes: a mini review. *3 Biotech*, **6**, 119.

Ito T., Yoshiguchi K., Ariesyady H. D. and Okabe S. (2012). Identification and quantification of key microbial trophic groups of methanogenic glucose degradation in an anaerobic digester sludge. *Bioresource Technology*, **123**, 599–607.

Janssen A. J.H., Sleyster R., van der Kaa C., Jochemsen A., Bontsema J. and Lettinga G. (1995). Biological sulphide oxidation in a fed-batch reactor. *Biotechnology and Bioengineering*, **47**, 327–333.

Janssen A. J.H., Meijer S., Bontsema J. and Lettinga G. (1998). Application of the redox potential for controling a sulfide oxidizing bioreactor. *Biotechnology and Bioengineering*, **60**, 147–155.

Jenicek P., Koubova J., Bindzar J. and Zabranska J. (2010). Advantages of anaerobic digestion of sludge in microaerobic conditions. *Water Science and Technology*, **62**(2), 427–434.

Jeppsson U. and Rosen C. (2006). Aspects on ADM1 Implementation within the BSM2 Framework.

Jimenez J., Latrille E., Harmand J., Robles A., Ferrer J., Gaida D., Wolf C., Mairet F., Bernard O., Alcaraz-Gonzalez V., Mendez-Acosta H., Zitomer D., Totzke D., Spanjers H., Jacobi F., Guwy A., Dinsdale R., Premier G., Mazhegrane S., Ruiz-Filippi G., Seco A., Ribeiro T., Pauss A. and Steyer J.-P. (2015). Instrumentation and control of anaerobic digestion processes: a review and some research challenges. *Reviews in Environmental Science andReviews in Environmental Science and Bio/Technology*, **14**, 615–648.

Jones B. D. and Ingle J. D. (2005). Evaluation of redox indicators for determining sulfate-reducing and dechlorinating conditions. *Water Research*, **39**, 4343–4354.

Kaksonen A. H. and Puhakka J. A. (2007). Sulfate Reduction Based Bioprocesses for the Treatment of Acid Mine Drainage and the Recovery of Metals. *Engineering in Life Sciences*, **7**, 541–564.

Kalyuzhnyi S., Fedorovich V., Lens P., Hulshoff Pol L. and Lettinga G. (1998). Mathematical modelling as a tool to study population dynamics between sulfate reducing and methanogenic bacteria. *Biodegradation*, **9**, 187–199.

Kazadi Mbamba C., Batstone D. J., Flores-Alsina X. and Tait S. (2015a). A generalised chemical precipitation modelling approach in wastewater treatment applied to calcite. *Water Research*, **68**, 342–353.

Kazadi Mbamba C., Tait S., Flores-Alsina X. and Batstone D. J. (2015b). A systematic study of multiple minerals precipitation modelling in wastewater treatment. *Water Research*, **85**, 359–370.

Kazadi Mbamba C. (2016). Dynamic modelling of Minerals Precipitation in Wastewater Treatment. The University of Queensland. https://doi.org/10.14264/uql.2016.350

Kazadi Mbamba C., Lindblom E., Flores-Alsina X., Tait S., Anderson S., Saagi R., Batstone D. J., Gernaey K. V. and Jeppsson U. (2019). Plant-wide model-based analysis of iron dosage strategies for chemical phosphorus removal in wastewater treatment systems. *Water Research*, **155**, 12–25.

Khanal S. K. and Huang J.-C. (2006). Online Oxygen Control for Sulfide Oxidation in Anaerobic Treatment of High-Sulfate Wastewater. *Water Environment Research*, **78**, 397–408.

Khoshnevisan B., Tsapekos P., Alfaro N., Díaz I., Fdz-Polanco M., Rafiee S. and Angelidaki I. (2017). A review on prospects and challenges of biological H_2S removal from biogas with focus on biotrickling filtration and microaerobic desulfurization. *Biofuel Research Journal*, **4**, 741–750.

Knobel A. N. and Lewis A. E. (2002). A mathematical model of a high sulphate wastewater anaerobic treatment system. *Water Research*, **36**, 257–265.

Kobayashi T., Li Y.-Y., Kubota K., Harada H., Maeda T. and Yu H.-Q. (2012). Characterization of sulfide-oxidizing microbial mats developed inside a full-scale anaerobic digester employing biological desulfurization. *Applied Microbiology and Biotechnology*, **93**, 847–857.

König J., Keesman K. J., Veeken A. and Lens P. N.L. (2006). Dynamic Modelling and Process Control of ZnS Precipitation. *Separation Science and Technology*, **41**, 1025–1042.

Koutsoukos P., Amjad Z., Tomson M. B. and Nancollas G. H. (1980). Crystallization of calcium phosphates. A constant composition study. *Journal of the American Chemical Society*, **102**, 1553–1557.

Kralj D., Brečević L. and Kontrec J. (1997). Vaterite growth and dissolution in aqueous solution III. Kinetics of transformation. *Journal of Crystal Growth*, **177**, 248–257.

Krayzelova L., Bartacek J., Kolesarova N. and Jenicek P. (2014). Microaeration for hydrogen sulfide removal in UASB reactor. *Bioresource Technology*, **172**, 297–302.

Krayzelova L., Bartacek J., Díaz I., Jeison D., Volcke E. I. P. and Jenicek P. (2015). Microaeration for hydrogen sulfide removal during anaerobic treatment: a review. *Reviews in Environmental Science and Bio/Technology*, **14**, 703–725.

Kurtz M. J. and Henson M. A. (1997). Input-output linearizing control of constrained nonlinear processes. *Journal of Process Control*, **7**, 3–17.

Lauwers J., Appels L., Thompson I. P., Degrève J., Van Impe J. F. and Dewil R. (2013). Mathematical modelling of anaerobic digestion of biomass and waste: Power and limitations. *Progress in Energy and Combustion Science*, **39**, 383–402.

Lee E., McCarty P. L., Kim J. and Bae J. (2016). Effects of $FeCl_3$ addition on the operation of a staged anaerobic fluidized membrane bioreactor (SAF-MBR). *Water Science and Technology*, **74**(1), 130–137.

Lens P. N. L. and Kuenen J. G. (2001). The biological sulfur cycle: Novel opportunities for environmental biotechnology. *Water Science and Technology*, **44**(8), 57–66.

Lewis A. E. (2010). Review of metal sulphide precipitation. *Hydrometallurgy*, **104**, 222–234.

Lewis A. E., Seckler M. M., Kramer H. and Van Rosmalen G. (2003). Industrial Crystallization in Practice from Process to Product, Cambridge University Press, UK.

Li Q. and Lancaster J. R. (2013). Chemical foundations of hydrogen sulfide biology. *Nitric Oxide*, **35**, 21–34.

Li Z.-Q., Liu G.-D., Duan L.-M., Shen G.-L. and Yu R.-Q. (1999). Sulfate-selective PVC membrane electrodes based on a derivative of imidazole as a neutral carrier. *Analytica Chimica Acta*, **382**, 165–170.

Li Y., Wang Y., Gao Y., Zhao H. and Zhou W. (2018). Seawater toilet flushing sewage treatment and nutrients recovery by marine bacterial-algal mutualistic system. *Chemosphere*, **195**, 70–79.

Liamleam W. and Annachhatre A. P. (2007). Electron donors for biological sulfate reduction. *Biotechnology Advances*, **25**, 452–463.

Liu Z., Maszenan A. M., Liu Y. and Ng W. J. (2015). A brief review on possible approaches towards controlling sulfate-reducing bacteria (SRB) in wastewater treatment systems. *Desalination and Water Treatment*, **53**, 2799–2807.

Lizarralde I., Fernández-Arévalo T., Brouckaert C., Vanrolleghem P., Ikumi D. S., Ekama G. A., Ayesa E. and Grau P. (2015). A new general methodology for incorporating physico-chemical transformations into multi-phase wastewater treatment process models. *Water Research*, **74**, 239–256.

Lizarralde I., Fernández-Arévalo T., Manas A., Ayesa E. and Grau P. (2019). Model-based opti mization of phosphorus management strategies in Sur WWTP, Madrid. *Water Research*, **153**, 39–52.

Lomako S. V., Astapovich R. I., Nozdrin-Plotnitskaya O. V., Pavlova T. E., Lei S., Nazarov V. A., Okaev E. B., Rakhman'ko E. M. and Egorov V. V. (2006). Sulfate-selective electrode and its application for sulfate determination in aqueous solutions. *Analytica Chimica Acta*, **562**, 216–222.

Lyew D. and Sheppard J. (2001). Use of conductivity to monitor the treatment of acid mine drainage by sulphate-reducing bacteria. *Water Research*, **35**, 2081–2086.

Majer V., Sedlbauer J. and Bergin G. (2008). Henry's law constant and related coefficients for aqueous hydrocarbons, CO_2 and H_2S over a wide range of temperature and pressure. *Fluid Phase Equilibria*, **272**, 65–74.

Martí N., Barat R., Seco A., Pastor L. and Bouzas A. (2017). Sludge management modeling to enhance P-recovery as struvite in wastewater treatment plants. *Journal of Environmental Management*, **196**, 340–346.

Mazloum Ardakani M., Akrami Z., Mansournia M. and Zare H. R. (2006). Sulfate-selective Electrode Based on a Complex of Copper. *Analytical Sciences*, **22**, 673–678.

Mazloum-Ardakani M., Manshadi A. D., Bagherzadeh M. and Kargar H. (2012). Impedimetric and Potentiometric Investigation of a Sulfate Anion-Selective Electrode: Experiment and Simulation. *Analytical Chemistry*, **84**, 2614–2621.

McDonagh C., Burke C. S. and MacCraith B. D. (2008). Optical Chemical Sensors. *Chemical Reviews*, **108**, 400–422.

McFarland M. J. and Jewell W. J. (1989). In situ control of sulfide emissions during the thermophilic (55°C) anaerobic digestion process. *Water Research*, **23**, 1571–1577.

Méndez-Acosta H. O., Palacios-Ruiz B., Alcaraz-González V., González-Álvarez V. and García-Sandoval J. P. (2010). A robust control scheme to improve the stability of anaerobic digestion processes. *Journal of Process Control*, **20**, 375–383.

Millero F. J. (1986). The thermodynamics and kinetics of the hydrogen sulfide system in natural waters. *Marine Chemistry*, **18**, 121–147.

Morigi M., Scavetta E., Berrettoni M., Giorgetti M. and Tonelli D. (2001). Sulfate-selective electrodes based on hydrotalcites. *Analytica Chimica Acta*, **439**, 265–272.

Musvoto E. V, Wentzel M. C., Loewenthal R. E. and Ekama G. A. (2000). Integrated chemical–physical processes modelling—I. Development of a kinetic-based model for mixed weak acid/base systems. *Water Research*, **34**, 1857–1867.

Muyzer G. and Stams A. J. M. (2008). The ecology and biotechnology of sulphate-reducing bacteria. *Nature Reviews Microbiology*, **6**, 441–454.

Nezamzadeh-Ejhieh A. and Afshari E. (2012). Modification of a PVC-membrane electrode by surfactant modified clinoptilolite zeolite towards potentiometric determination of sulfide. *Microporous and Mesoporous Materials*, **153**, 267–274.

Nezamzadeh-Ejhieh A. and Esmaeilian A. (2012). Application of surfactant modified zeolite carbon paste electrode (SMZ-CPE) towards potentiometric determination of sulfate. *Microporous and Mesoporous Materials*, **147**, 302–309.

Nghiem L. D., Manassa P., Dawson M. and Fitzgerald S. K. (2014). Oxidation reduction potential as a parameter to regulate micro-oxygen injection into anaerobic digester for reducing hydrogen sulphide concentration in biogas. *Bioresource Technology*, **173**, 443–447.

Nguyen D. and Khanal S. K. (2018). A little breath of fresh air into an anaerobic system: How microaeration facilitates anaerobic digestion process. *Biotechnology Advances*, **36**, 1971–1983.

Nguyen D., Gadhamshetty V., Nitayavardhana S. and Khanal S. K. (2015). Automatic process control in anaerobic digestion technology: A critical review. *Bioresource Technology*, **193**, 513–522.

Nguyen D., Wu Z., Shrestha S., Lee P. H., Raskin L. and Khanal S. K. (2019). Intermittent micro-aeration: New strategy to control volatile fatty acid accumulation in high organic loading anaerobic digestion. *Water Research*, **166**, 115080.

Nishizawa S., Bühlmann P., Xiao K. P. and Umezawa Y. (1998). Application of a bis-thiourea ionophore for an anion selective electrode with a remarkable sulfate selectivity. *Analytica Chimica Acta*, **358**, 35–44.

Noguera D. R., Brusseau G. A., Rittmann B. E. and Stahl D. A. (1998). A unified model describing the role of hydrogen in the growth of *Desulfovibrio vulgaris* under different environmental conditions. *Biotechnology and Bioengineering*, **59**(6), 732–746.

Noguera D. R., Pizarfo G., Stahl D. A. and Rittmann B. E. (1999). Simulation of multispecies biofilm development in three dimensions. *Water Science and Technology*, **39**(7), 123–130.

Olsson G., Carlsson B., Comas J., Copp J., Gernaey K. V., Ingildsen P., Jeppsson U., Kim C., Rieger L., Rodríguez-Roda I., Steyer J.-P., Takács I., Vanrolleghem P. A., Vargas A., Yuan Z. and Åmand L. (2014). Instrumentation, control and automation in wastewater – from London 1973 to Narbonne 2013. *Water Science and Technology*, **69**(7), 1373.

Overmeire A., Lens P. and Verstraete W. (1994). Mass transfer limitation of sulfate in methanogenic aggregates. *Biotechnology and Bioengineering*, **44**, 387–391.

Pandey S. K., Kim K.-H. and Tang K.-T. (2012). A review of sensor-based methods for monitoring hydrogen sulfide. *TRAC Trends in Analytical Chemistry*, **32**, 87–99.

Patón M., González-Cabaleiro R. and Rodríguez J. (2018). Activity corrections are required for accurate anaerobic digestion modelling. *Water Science and Technology*, **77**(8), 2057–2067.

Peces M., Astals S., Jensen P. D. and Clarke W. P. (2018). Deterministic mechanisms define the long-term anaerobic digestion microbiome and its functionality regardless of the initial microbial community. *Water Research*, **141**, 366–376.

Percheron, G., Bernet, N. and Moletta, R. (1996). A new method for the determination of dissolved sulfide in strongly colored anaerobically treated effluents. *Bioprocess Engineering*. **15**(6), 317–322.

Poinapen J. and Ekama G. (2010). Biological sulphate reduction with primary sewage sludge in an upflow anaerobic sludge bed reactor – Part 6: Development of a kinetic model for BSR. *Water SA*, **36**, 203–214.

Pokorna-Krayzelova L., Mampaey K. E., Vannecke T. P. W., Bartacek J., Jenicek P. and Volcke E. I. P. (2017). Model-based optimization of microaeration for biogas desulfurization in UASB reactors. *Biochemical Engineering Journal*, **125**, 171–179.

Premier G. C., Dinsdale R., Guwy A. J., Hawkes F. R., Hawkes D. L. and Wilcox S. J. (1999). A comparison of the ability of black box and neural network models of ARX structure to represent a fluidized bed anaerobic digestion process. *Water Research*, **33**, 1027–1037.

Puyol D., Batstone D. J., Hülsen T., Astals S., Peces M. and Krömer J. O. (2017). Resource recovery from wastewater by biological technologies: Opportunities, challenges, and prospects. *Frontiers in Microbiology*, **7**, 1–23.

Ramos I. and Fdz-Polanco M. (2014). Microaerobic control of biogas sulphide content during sewage sludge digestion by using biogas production and hydrogen sulphide concentration. *Chemical Engineering Journal*, **250**, 303–311.

Ramos I., Pérez R. and Fdz-Polanco M. (2014). The headspace of microaerobic reactors: Sulphide-oxidising population and the impact of cleaning on the efficiency of biogas desulphurisation. *Bioresource Technology*, **158**, 63–73.

Ramsing N. B., Kühl M. and Jørgensen B. B. (1993). Distribution of sulfate-reducing bacteria, O_2, and H_2S in photosynthetic biofilms determined by oligonucleotide probes and microelectrodes. *Applied and Environmental Microbiology*, **59**, 3840–3849.

Redondo R., Machado V. C., Baeza M., Lafuente J. and Gabriel D. (2008). On-line monitoring of gas-phase bioreactors for biogas treatment: hydrogen sulfide and sulfide analysis by automated flow systems. *Analytical and Bioanalytical Chemistry*, **391**, 789–798.

Renard P., Dochain D., Bastin G., Naveau H. and Nyns E.-J. (1988). Adaptive control of anaerobic digestion processes – a pilot-scale application. *Biotechnology and Bioengineering*, **31**, 287–294.

Robles Á., Ruano M. V., Charfi A., Lesage G., Heran M., Harmand J., Seco A., Steyer J.-P., Batstone D. J., Kim J. and Ferrer J. (2018). A review on anaerobic membrane bioreactors (AnMBRs) focused on modelling and control aspects. *Bioresource Technology*, **270**, 612–626.

Salehin S., Kulandaivelu J., Rebosura M., Khan W., Wong R., Jiang G., Smith P., McPhee P., Howard C., Sharma K., Keller J., Donose B. C., Yuan Z. and Pikaar I. (2019). Opportunities for reducing coagulants usage in urban water management: The Oxley Creek Sewage Collection and Treatment System as an example. *Water Research*, **165**, 114996.

Sampaio R. M. M., Timmers R. A., Xu Y., Keesman K. J. and Lens P. N. L. (2009). Selective precipitation of Cu from Zn in a pS controlled continuously stirred tank reactor. *Journal of Hazardous Materials*, **165**, 256–265.

Sampaio R. M. M., Timmers R. A., Kocks N., André V., Duarte M. T., van Hullebusch E. D., Farges F. and Lens P. N. L. (2010). Zn–Ni sulfide selective precipitation: The role of supersaturation. *Separation and Purification Technology*, **74**, 108–118.

Santegoeds C. M., Damgaard L. R., Hesselink G., Zopfi J., Lens P., Muyzer G. and de Beer D. (1999). Distribution of sulfate-reducing and methanogenic bacteria in anaerobic aggregates determined by microsensor and molecular analyses. *Applied and Environmental Microbiology*, **65**, 4618–4629.

Seco A., Ruano M. V, Ruiz-Martinez A., Robles A., Barat R., Serralta J. and Ferrer J. (2020). Plant-wide modelling in wastewater treatment: showcasing experiences using the Biological Nutrient Removal Model. *Water Science and Technology*, **81**(8), 1700–1714. https://doi.org/10.2166/wst.2020.056

Serrano A., Peces M., Astals S. and Villa-Gómez D. K. (2020). Batch assays for biological sulfate-reduction: a review towards a standardized protocol. *Critical Reviews in Environmental Science and Technology*, **50**, 1195–1223.

Shakeri Yekta S., Ziels R. M., Björn A., Skyllberg U., Ejlertsson J., Karlsson A., Svedlund M., Willén M. and Svensson B. H. (2017). Importance of sulfide interaction with iron as regulator of the microbial community in biogas reactors and its effect on methanogenesis, volatile fatty acids turnover, and syntrophic long-chain fatty acids degradation. *Journal of Bioscience and Bioengineering*, **123**, 597–605.

Shamsipur M., Yousefi M., Hosseini M., Ganjali M. R., Sharghi H. and Naeimi H. (2001). A Schiff Base Complex of Zn(II) as a Neutral Carrier for Highly Selective PVC Membrane Sensors for the Sulfate Ion. *Analytical Chemistry*, **73**, 2869–2874.

Shen C. F. and Guiot S. R. (1996). Long-term impact of dissolved O_2 on the activity of anaerobic granules. *Biotechnology and Bioengineering*, **49**, 611–620.

Solon K., Flores-Alsina X., Mbamba C. K., Volcke E. I. P., Tait S., Batstone D., Gernaey K. V. and Jeppsson U. (2015). Effects of ionic strength and ion pairing on (plant-wide) modelling of anaerobic digestion. *Water Research*, **70**, 235–245.

Solon K., Flores-Alsina X., Kazadi Mbamba C., Ikumi D., Volcke E. I.P., Vaneeckhaute C., Ekama G., Vanrolleghem P. A., Batstone D. J., Gernaey K. V. and Jeppsson U. (2017). Plant-wide modelling of phosphorus transformations in wastewater treatment systems: Impacts of control and operational strategies. *Water Research*, **113**, 97–110.

Stewart P. S. (1998). A review of experimental measurements of effective diffusive permeabilities and effective diffusion coefficients in biofilms. *Biotechnology and Bioengineering*, **59**, 261–272.

Steyer J.-P., Buffière P., Rolland D. and Moletta R. (1999). Advanced control of anaerobic digestion processes through disturbances monitoring. *Water Research*, **33**, 2059–2068.

Steyer J. P., Bernard O., Batstone D. J. and Angelidaki I. (2006). Lessons learnt from 15 years of ICA in anaerobic digesters. *Water Science and Technology*, **53**(4–5), 25–33.

Sun J., Dai X., Wang Q., Pan Y. and Ni B.-J. (2016). Modelling Methane Production and Sulfate Reduction in Anaerobic Granular Sludge Reactor with Ethanol as Electron Donor. *Scientific Reports*, **6**, 35312.

Tartakovsky B., Mehta P., Bourque J.-S. and Guiot S. R. (2011). Electrolysis-enhanced anaerobic digestion of wastewater. *Bioresource Technology*, **102**, 5685–5691.

Tigli O. and Zaghloul M. E. (2007). A Novel Saw Device in CMOS: Design, Modeling, and Fabrication. *Ieee Sensors Journal*, **7**, 219–227.

Tóth I., Solymosi P. and Szabó Z. (1988). Application of a sulphide-selective electrode in the absence of a pH-buffer. *Talanta* **35**, 783–788.

van Lier J. B., van der Zee F. P., Frijters C. T. M. J. and Ersahin M. E. (2015). Celebrating 40 years anaerobic sludge bed reactors for industrial wastewater treatment. *Reviews in Environmental Science and Bio/Technology*, **14**, 681–702.

Vavilin V. A., Vasiliev V. B., Ponomarev A. V. and Rytow S. V. (1994). Simulation model 'methane' as a tool for effective biogas production during anaerobic conversion of complex organic matter. *Bioresource Technology*, **48**, 1–8.

Vavilin V. A., Vasiliev V. B., Rytov S. V. and Ponomarev A. V. (1995). Modeling ammonia and hydrogen sulfide inhibition in anaerobic digestion. *Water Research*, **29**, 827–835.

Veeken A. H. M., de Vries S., van der Mark A. and Rulkens W. H. (2003). Selective Precipitation of Heavy Metals as Controlled by a Sulfide Selective Electrode. *Separation Science and Technology*, **38**, 1–19.

Villa-Gomez D. K. K., Cassidy J., Keesman K. J. J., Sampaio R. and Lens P. N. L. (2014). Sulfide response analysis for sulfide control using a pS electrode in sulfate reducing bioreactors. *Water Research*, **50**, 48–58.

Virji S., Fowler J. D., Baker C. O., Huang J., Kaner R. B. and Weiller B. H. (2005). Polyaniline nanofiber composites with metal salts: Chemical sensors for hydrogen sulfide. *Small* **1**, 624–627.

Wan Y., Zhang D. and Hou B. (2009). Monitoring microbial populations of sulfate-reducing bacteria using an impedimetric immunosensor based on agglutination assay. *Talanta* **80**, 218–223.

Wan Y., Zhang D. and Hou B. (2010a). Determination of sulphate-reducing bacteria based on vancomycin-functionalised magnetic nanoparticles using a modification-free quartz crystal microbalance. *Biosensors & Bioelectronics*, **25**, 1847–1850.

Wan Y., Zhang D. and Hou B. (2010b). Selective and specific detection of sulfate-reducing bacteria using potentiometric stripping analysis. *Talanta*, **82**, 1608–1611.

Wan Y., Zhang D., Wang Y., Qi P. and Hou B. (2011). Direct immobilisation of antibodies on a bioinspired architecture as a sensing platform. *Biosensors & Bioelectronics*, **26**, 2595–2600.

Ward A. J., Hobbs P. J., Holliman P. J. and Jones D. L. (2008). Optimisation of the anaerobic digestion of agricultural resources. *Bioresource Technology*, **99**, 7928–7940.

Wilcox S. J., Hawkes D. L., Hawkes F. R. and Guwy A. J. (1995). A neural network, based on bicarbonate monitoring, to control anaerobic digestion. *Water Research*, **29**, 1465–1470.

Wu D., Ekama G. A., Chui H.-K., Wang B., Cui Y.-X., Hao T.-W., van Loosdrecht M. C. M. and Chen G.-H. (2016). Large-scale demonstration of the sulfate reduction autotrophic denitrification nitrification integrated (SANI®) process in saline sewage treatment. *Water Research*, **100**, 496–507.

Wu D., Li L., Zhao X., Peng Y., Yang P. and Peng X. (2019). Anaerobic digestion: A review on process monitoring. *Renewable and Sustainable Energy Reviews*, **103**, 1–12.

Yang Y., Chen Q., Guo J. and Hu Z. (2015). Kinetics and methane gas yields of selected C1 to C5 organic acids in anaerobic digestion. *Water Research*, **87**, 112–118.

Zadeh L. A. (1965). Fuzzy sets. *Information and Control*, **8**, 338–353.

Zhang L., De Schryver P., De Gusseme B., De Muynck W., Boon N. and Verstraete W. (2008). Chemical and biological technologies for hydrogen sulfide emission control in sewer systems: A review. *Water Research*, **42**, 1–12.

Zancato, M., Pietrogrande, A. and Macca, C. (1990). Sequential determination of sulfur and chlorine in organic compounds by potentiometric titration of sulfate and chloride with an automatic titrator. *Annali di Chimica*, **80**(9–10), 445–452.